

# Important Notice

This copy may be used only for the purposes of research and private study, and any use of the copy for a purpose other than research or private study may require the authorization of the copyright owner of the work in question. Responsibility regarding questions of copyright that may arise in the use of this copy is assumed by the recipient.

DEC - 7 1989

THE UNIVERSITY OF CALGARY

GALLAGHER LIBRARY  
UNIVERSITY OF CALGARY  
CALGARY, ALBERTA  
CANADA T2N 1N4

**SEISMIC REFLECTION IMAGING OF THE CHAPLEAU BLOCK,  
KAPUSKASING STRUCTURAL ZONE, ONTARIO**

by

Wayne T. Geis

A THESIS  
SUBMITTED TO THE FACULTY OF GRADUATE STUDIES  
IN PARTIAL FULFILLMENT OF THE REQUIREMENTS FOR THE  
DEGREE OF MASTER OF SCIENCE

DEPARTMENT OF GEOLOGY AND GEOPHYSICS

CALGARY, ALBERTA

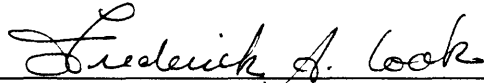
AUGUST, 1989

© W.T. Geis, 1989

THE UNIVERSITY OF CALGARY

FACULTY OF GRADUATE STUDIES

The undersigned certify that they have read and recommend to the Faculty of Graduate Studies for acceptance, a thesis entitled "Seismic reflection imaging of the Chapleau block, Kapuskasing Structural Zone, Ontario" submitted by Wayne T. Geis in partial fulfillment of the requirements for the degree of Master of Science.



---

Supervisor, Dr. F.A. Cook  
Department of Geology and Geophysics



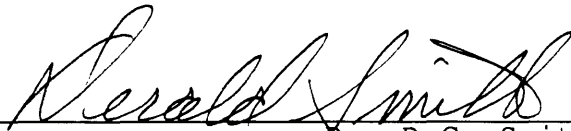
---

Dr. D.R.M. Pattison  
Department of Geology and Geophysics



---

Dr. D.C. Lawton  
Department of Geology and Geophysics



---

Dr. D.G. Smith  
Department of Geography

August 30, 1989

## ABSTRACT

The granulite and upper amphibolite grade rocks of the Kapuskasing structural zone (KSZ) in Ontario represent an exposure of Archean crust that has been uplifted along a southeast verging thrust fault system. Regional and high resolution seismic reflection data recorded across the structure by LITHOPROBE image at least three low angle thrust faults that merge into a flat detachment towards the northwest. Along an east-west transect across the southern end of the KSZ the seismic geometry resembles a 'ramp and flat' style of thrusting, resulting in a thin upper plate above the 15-17 km (about 5.0 s two-way time) detachment. Other seismic profiles provide regional three dimensional coverage, allowing construction of time structure maps of the principal fault surface. These maps show that, on a regional scale, the time contours generally parallel the surface expression of the fault(s), the Ivanhoe Lake fault zone (ILFZ). Large structures imaged beneath the adjacent Abitibi belt also roughly parallel the ILFZ, suggesting they may have controlled the emplacement of the KSZ or are possibly deeper level detachments associated with the formation of the KSZ. Coupled with the surface geology and available geobarometry, three conceptual models are proposed that are consistent with the seismic geometry, but

differ in respect to which of the faults is the principal detachment and where potential ramps are placed. From these models estimates of the minimum amount of horizontal shortening range between 55 and 85 km in a NW-SE direction. This large amount of shortening implies that much of the upper-middle crust of Superior province was detached from the lower crust during the formation of the KSZ. The proposed geometric interpretation, which includes ramps, flats and imbricate thrusts, further implies that rocks deep within the crust may deform into structures that strongly resemble those in layered media such as sediments in Phanerozoic supra-crustal fold and thrust belts.

In addition to characterizing the geometric information from the reflection data, acquisition of data with both high resolution and regional parameters along a 17 km segment of line allowed a comparison of these two modes of recording. The initial stacked section of the data recorded with regional parameters indicated that the high resolution data provided a far superior image to that of the regional data. However, reprocessing of the regional data with parameters that are comparable to the high resolution profile, reveals that significant improvements can be made on the regional profile image quality. A short offset range and a correlation statics window that encompasses early arrivals are the two most important considerations when imaging dipping shallow structures.

## ACKNOWLEDGEMENTS

I am deeply indebted to my supervisor, Dr. Fred Cook for his exceptional scientific guidance, inspiration and for all the opportunities the Lithoprobe project has given me. Thanks Fred for showing me there is more to seismic exploration than salt domes, reefs and sand channels.

Drs. Alan Green and John Percival of the Geological Survey of Canada provided many helpful comments and shared their enthusiasm for the Kapuskasing project.

John Varsek provided many stimulating scientific and philosophical discussions which have helped put my role as a geophysicist into perspective.

Kevin Coflin's trail blazing efforts in learning new software packages has certainly made my research easier.

Special thanks to Paulette Campbell for constant encouragement and for most of all making life enjoyable during the difficult periods of my M.Sc. program.

None of this work would be possible if not for my parents, Stan and Joyce Geis, who encouraged and supported my education. Thanks mom and dad for all the sacrifices you have made during the past 25 years.

This thesis is dedicated to my grandmother, Magdalene Stephens. When I was a child she bought me a book on the inner Earth and read it to me because it was "too advanced".

## TABLE OF CONTENTS

APPROVAL PAGE.....	ii
ABSTRACT.....	iii
ACKNOWLEDGEMENTS.....	v
DEDICATION.....	vi
TABLE OF CONTENTS.....	vii
LIST OF TABLES.....	x
LIST OF FIGURES.....	xi
CHAPTER-1: INTRODUCTION.....	1
Why study the Kapuskasing structure?.....	2
Objectives of this research.....	4
CHAPTER-2: BACKGROUND AND PREVIOUS WORK.....	9
Regional setting.....	9
Evolution of thought in the interpretation of the KSZ.....	10
Tectonic framework of the KSZ.....	11
Age of Uplift.....	15
Comparison with Rocky Mountain structures.....	16
CHAPTER-3: SEISMIC DATA BASE.....	19
Seismic data acquisition.....	19



Seismic data processing.....	22
Coherency filtering.....	22
<b>CHAPTER-4: REPROCESSING OF LINE 2 REGIONAL.....</b>	<b>30</b>
Introduction.....	30
Standard reprocessing comparison.....	35
Additional signal enhancement.....	42
Summary of Chapter 4.....	60
<b>CHAPTER-5: THIN THRUST SHEET FORMATION           OF THE KSZ.....</b>	<b>62</b>
Introduction.....	62
Local geology along the seismic profiles.....	62
Data description and interpretation.....	65
Line 2 high resolution.....	65
East-west regional data.....	73
Discussion and implications of a thin thrust sheet model.....	79
Summary of Chapter 5.....	82
<b>CHAPTER-6: THREE DIMENSIONAL STRUCTURE OF THE           CHAPLEAU BLOCK.....</b>	<b>84</b>
Introduction.....	84
Data description.....	84
Line 1.....	86
Line 6.....	89
Line 5.....	92

3-D Geometry of Kapuskasing thrust block.....	92
Some comments on the Abitibi belt reflections.....	95
Summary of Chapter 6.....	100
<b>CHAPTER-7: RECONSTRUCTIONS.....</b>	<b>101</b>
Introduction.....	101
Constraints.....	102
Conceptual models.....	104
Models 1 and 2.....	104
Model 3.....	107
Summary of Chapter 7.....	110
<b>CHAPTER-8: CONCLUSIONS.....</b>	<b>112</b>
Recommendations for future work.....	114
<b>REFERENCES.....</b>	<b>116</b>

## LIST OF TABLES

Table 3.1:	Regional data acquisition parameters.....	20
Table 3.2:	High resolution data acquisition parameters.....	21
Table 3.3:	Regional data processing parameters.....	23
Table 3.4:	High resolution data processing parameters.....	24

## FIGURE CAPTIONS

Figure 1.1:	Map of local geology from the southern KSZ showing the location of seismic lines.....	8
Figure 2.1:	Crustal cross section of the KSZ.....	12
Figure 2.2:	Tectonic framework of the KSZ.....	14
Figure 2.3:	Comparison with Rocky Mountain structures.....	18
Figure 3.1:	Coherency filtering example.....	29
Figure 4.1:	Line 2 regional original processing.....	32
Figure 4.2:	Line 2 high resolution original processing.....	34
Figure 4.3:	Shot gather from V.P. 189.....	37
Figure 4.4:	Shot gather form V.P. 191.....	39
Figure 4.5:	Summation of shot gathers.....	41
Figure 4.6:	Reprocessing of regional data.....	44
Figure 4.7:	High resolution data band limited.....	47
Figure 4.8:	Reprocessed regional data band limited.....	49
Figure 4.9:	Reprocessed version of regional data with high resolution parameters.....	53
Figure 4.10:	Amplitude spectra comparison.....	55
Figure 4.11:	Spectral balanced version of regional data.....	58
Figure 4.12:	Amplitude spectra after spectral balancing.....	59

Figure 5.1:	Surface geology along Line 2.....	64
Figure 5.2:	Line 2 high resolution.....	67
Figure 5.3:	Line 2 high resolution with faults interpreted.....	70
Figure 5.4:	Geologic cross section beneath Line 2.....	72
Figure 5.5:	Seismic data across east-west transect.....	76
Figure 5.6:	Thin thrust sheet interpretation.....	78
Figure 6.1:	Seismic data along Line 1.....	88
Figure 6.2:	Seismic data along Line 6.....	91
Figure 6.3:	Seismic data along Line 5.....	94
Figure 6.4:	Isochron map of fault-1.....	96
Figure 6.5:	Perspective view of fault-1 surface.....	97
Figure 6.6:	Isochron map of Abitibi belt reflection.....	99
Figure 7.1:	Model-1.....	105
Figure 7.2:	Refraction velocity profile.....	106
Figure 7.3:	Model-2.....	108
Figure 7.4:	Model-3.....	109

## CHAPTER 1: INTRODUCTION

Broad exposures of high grade granulite facies rocks are interpreted by some as uplifted portions of the deep crust. Several well documented regions include the Ivrea zone of the southern Alps (Fountain and Salisbury, 1981), the Limpopo belt in southern Africa (Coward and Fairhead, 1980), and the Dharwar craton in southern India (Raase et al, 1986). In the Canadian shield the granulite and upper amphibolite grade rocks of the Kapuskasing structural zone (KSZ) cut obliquely across lower grade belts of the Archean Superior province (Figure 1.1) and are interpreted to represent an exposure of middle to lower crust that was uplifted along a southeast-verging thrust fault of possible Early Proterozoic age (Percival and Card, 1983, 1985; Cook, 1985; Percival and McGrath, 1986).

The subsurface structural geometry of the fault and related features have not been well known until now. However, new LITHOPROBE seismic reflection data provide evidence for the existence of at least three thrust faults underlying the KSZ, all of which are low angle and likely merge into a flat detachment that may ramp deep into the crust some distance west of the uplifted block (Geis et al., 1989). The geometry thus resembles a 'ramp and flat' style of thrust faulting, resulting in a thin upper plate

above the detachment. This is a surprising and significant discovery as previous models have suggested that the fault is high angle and extends to lower crustal depths in excess of 30 km (Percival and Card, 1983; Cook, 1985; Percival and McGrath, 1986).

### **Why Study the Kapuskasing Structure?**

According to some estimates, as much as 70 percent of the existing continental crust was formed by the end of the Archean (2.5 Ga; e.g. Kroner, 1981; Brown and Musset, 1984). However, controversy surrounds our understanding of the processes that controlled early continental growth. For example, were the tectonic processes operating in the Archean and Early Proterozoic similar to those in the Phanerozoic? Much of the debate centers around whether early continental crust was constructed vertically by processes of differentiation and associated vertical uplift, by progressive lateral accretion of magmatic arcs, or by some process unique to the Archean (see Kroner, 1981; Brown and Mussett, 1984 and Nisbet, 1987 for a general discussion on Archean geology and early crustal evolution). The lower crustal rocks of the KSZ thus provide a rare window for study of the structure and composition of

Archean crust to a paleo-depth of 25 km (Percival, 1983).

Many topics of both global and regional importance concerning early crustal evolution can be addressed by studying the rocks within the Kapuskasing structure. For example, seismic reflection imaging is a powerful technique that allows the structures responsible for the uplift of rock units observed at the surface to be traced into the deep crust. Thus, the determination of the depth and geometry of faults and related structures may have important implications for Late Archean-Early Proterozoic tectonic models and crustal rheology.

The formation of the KSZ likely played a prominent role in the evolution of the Superior province, which is the world's largest Archean craton. In the region under study here the KSZ divides the Superior province into two similar granite-greenstone terranes, the Abitibi and Wawa subprovinces (Figure 1.1). Estimates of the amount of horizontal shortening along the faults associated with the KSZ will be useful in constraining the tectonic history of the region.

The causes of deep crustal reflections is a topic of wide interest. Most deep seismic profiles contain lower crustal reflections, but only in a few cases can they be positively identified. Speculated causes for these reflections include lithological layering, mylonite zones, and zones of high pore fluid pressure (e.g. Fountain et al,



1984; Jones and Nur, 1984; Barazangi and Brown, 1986a, 1986b; Christensen and Szymanski, 1988). In the KSZ, many reflections can be traced to within 200-300 m of the surface where correlation with observed geologic layering allows almost certain identification.

### **Objectives of This Study**

The seismic lines (Figure 1.1) used in this study cross the southern portion of the KSZ (Chapleau Block; Percival and McGrath, 1986;) and include both regional and high resolution data (line 2). The seismic images provide strong geometric constraints on the evolution of the KSZ, and establish a framework for the interpretation of other geological and geophysical data acquired as part of the LITHOPROBE Kapuskasing project.

There are two primary objectives in this thesis research. The first is to interpret and discuss the implications of the seismic reflection geometry of the structures beneath the Chapleau block of the KSZ. The second is to investigate the reasons for an apparent difference between data sets recorded with high resolution and regional parameters.

Using the data along the east-west transect (lines 2, 3

and 4) the thin thrust sheet formation of the KSZ is discussed in Chapter 5. This transect best represents the thin thrust sheet geometry and includes the high resolution profile, which provides excellent correlation to the surface geology. The seismic data cross the structure in several different directions (Figure 1.1). Therefore, by incorporating the remaining profiles, the 3-D geometry of the principal faults beneath the structure is presented in Chapter 6. With the assistance of a Landmark Graphics Interpretational Workstation, time structure maps of the Kapuskasing thrust block have been constructed allowing its true orientation in the subsurface to be estimated. In addition a speculative interpretation is made of reflections observed in the adjacent Abitibi belt. In Chapter 7 the main features from the seismic geometry beneath the KSZ are used to produce simple reconstructions of the thrust sheets. The implications of the reconstructions are also discussed in this chapter.

The reprocessing of regional line 2 is discussed in Chapter 4. The stack section produced from the original processing of regional line 2 is of apparently poorer quality than high resolution line 2, particularly for shallow, steeply dipping reflections. Although it was suspected that this difference was partly due to a prestack summation of adjacent shot gathers prior to the initial processing, careful reprocessing shows that the prestack

summation only has a minor effect. Enhancement of shallow data using a variety of carefully chosen parameters shows that the regional data can produce stack sections that are nearly identical to the high resolution data for similar frequency bands.

Figure 1.1: (next page) Generalized geologic map of the southern portion of the Chapleau block of the KSZ (after Percival and Card, 1983). Shown are the six seismic lines recorded as part of the LITHOPROBE project. Inset is a generalized map of the Archean Superior Province in the central Canadian Shield. The NNE trending KSZ cross-cuts the east-west trending subprovinces of the Superior province.



## CHAPTER 2: BACKGROUND AND PREVIOUS WORK

### Regional Setting

The east-west structural trends of metavolcanic and metasedimentary belts of the Archean Superior province (Figure 1.1) are cross-cut by the NNE trending KSZ. Along the southern end (Figure 1.1) of the structure, metamorphic grade increases easterly from greenschist facies rocks in Michipicoten belt, to amphibolite facies in the Wawa gneiss terrane and finally into granulite facies within the Kapuskasing zone (Percival and Card, 1983). High grade rocks of the KSZ are separated from the low grade Abitibi subprovince to the east by the Ivanhoe Lake fault zone (ILFZ; Figure 1.1), which contains fault-related rocks including cataclasite, pseudotachylite, mylonite and blastomylonite (Percival and Card, 1983, 1985; Bursnall, 1989). The ILFZ has been traditionally referred to as the Ivanhoe Lake cataclastic zone (ILCZ); however with the recent discovery of significant amounts of rocks deformed under ductile conditions (mylonite), the more generic name, ILFZ has been adopted (Bursnall, 1989). Associated with the exposures of high grade rocks are prominent gravity and magnetic anomalies that extend from Lake Superior in the

south to James Bay in the north (Garland, 1950; Innes et al, 1967).

### **Evolution of Thought in the Interpretation of the KSZ**

For several decades the KSZ has been known to be a prominent and somewhat enigmatic structure within the Superior province. Early interpretations included a thinning of the granitic crustal layer (Garland, 1950), a graben associated with mid-Proterozoic rifting (Innes et al, 1967), a Proterozoic suture zone (Wilson, 1968), a horst structure (McGlynn, 1970), and a failed arm of the Keweenawan rift system (Burke and Dewey, 1973). A later interpretation suggested a zone of large sinistral transcurrent shear (Watson, 1980). However, the current accepted interpretation is that of Percival and Card (1983), in which uplift due to an east-verging crustal scale thrust fault exposed an oblique cross section of the lower crust (Figure 2.1). This model is supported by:

- 1) The west to east increase in metamorphic grade to granulite facies within the KSZ, then an abrupt return to low grade in the Abitibi belt across the ILFZ. Geobarometric measurements indicate pressures from 2-3 kbar

(200-300 MPa) in the greenschist rocks of the Michipicoten belt, through 4-5 kbar (400-500 MPa) amphibolite facies tonalite gneiss in the Wawa belt, to 6-9 kbar (600-900 MPa) granulites of the Kapuskasing zone (Percival and McGrath, 1986).

2) The east to west increase in the Bouguer gravity between the generally lower density Abitibi rocks and higher density KSZ rock across the ILFZ, in which modeling is consistent with a west dipping crustal slab (Figure 2.1; Percival and Card, 1983).

3) The presence of west dipping reflections projecting to the surface in the vicinity of the ILFZ (Cook, 1985; Geis et al., 1988), suggesting that reverse faults juxtapose the high grade KSZ rocks over lower grade Abitibi belt rocks.

### **Tectonic Framework of the KSZ**

The NNE trending KSZ consists of three tectonic blocks of distinct geological and geophysical character (Percival and McGrath, 1986). From south to north, these include the Chapleau, Groundhog River and the Fraserdale-Moosonee blocks (Figure 2.2).



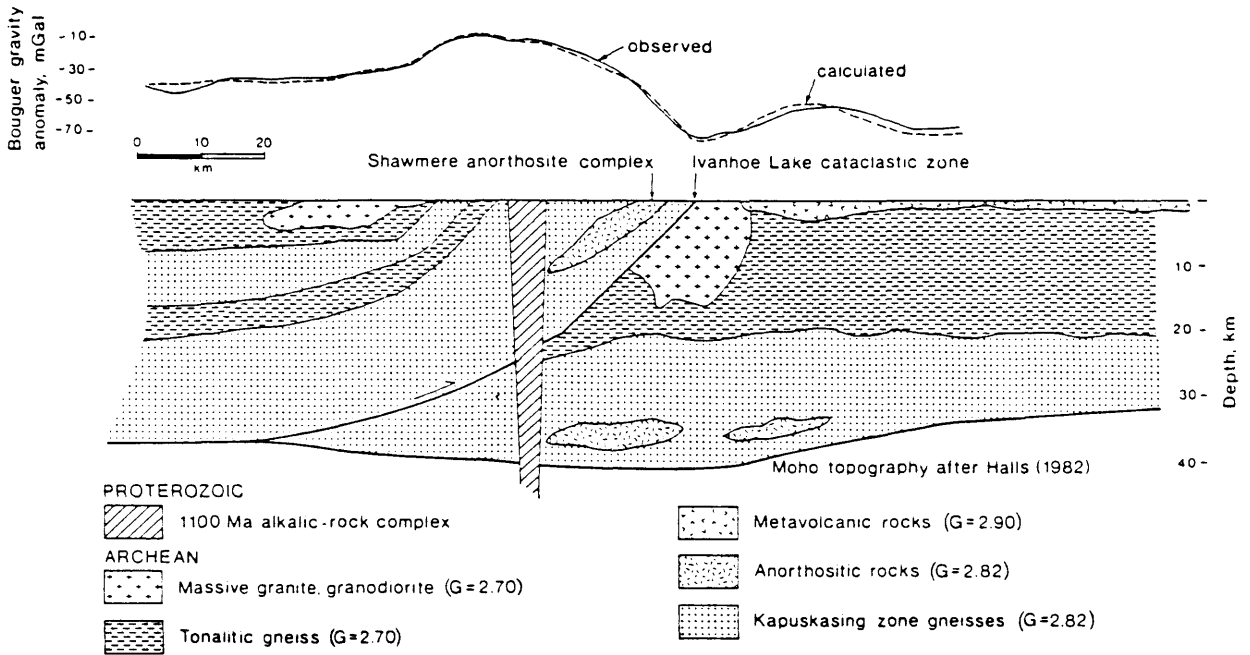


Figure 2.1: Generalized cross section of Percival and Card (1985 p. 186), showing the single high angle crustal scale thrust fault thought by them to have been responsible for the emplacement of the middle to lower crustal rocks.

The Chapleau block is bounded on the east by the ILFZ, on the west by the Saganash Lake fault (SLF), a post thrusting extensional fault, and is separated from the Groundhog River block by the northwest side down Wakusimi River fault (Leclair and Poirier, 1989). The block contains predominantly tonalitic orthogneiss, the Shawmere anorthosite complex, and minor amounts of paragneiss and mafic gneiss (Percival and Card, 1983).

The Groundhog River block is believed to be the northward continuation of the Chapleau block, but the aeromagnetic expression changes abruptly across the Wakusimi River fault (Figure 2.2; Percival and McGrath, 1986). The block contains tonalitic orthogneiss, mafic gneiss and rare paragneiss (Percival and Card, 1983). The Groundhog River block is separated from the Fraserdale-Moosonee block to the northeast by a 65 km gap of lower grade rocks that are characteristic of the Wawa belt.

The Fraserdale-Moosonee block is bounded on the east by the Bad River fault, which is likely a northern extension of the ILFZ, and on the west by the post thrusting Foxville and Kineras faults. The rock types consist mainly of metasedimentary granulites, with some tonalite and a little mafic gneiss (Percival and McGrath, 1986).

It is postulated that a 500 km long NNE trending system of thrust faults, which includes the ILFZ and the Bad River faults, emplaced the granulite facies rocks of the KSZ at

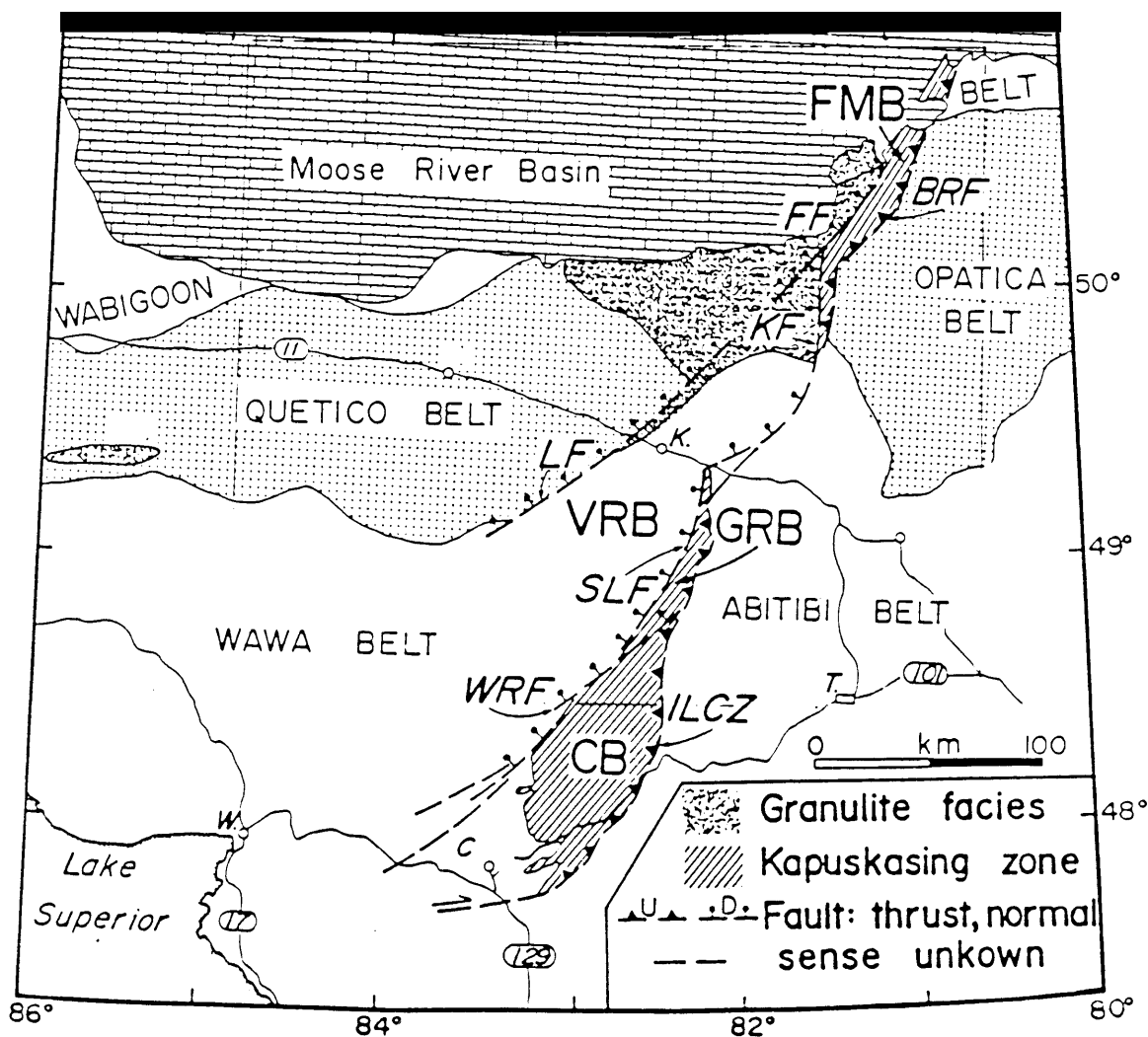


Figure 2.2: Regional geology of central Superior Province showing the major tectonic elements of the KSZ including the Chapleau, the Groundhog River (GRB) and the Fraserdale-Moosonee (FMB) blocks. Faults include the ILCZ (or ILFZ), the Saganash Lake (SLF), the Wakusimi River (WRF), the Bad River (BRF), the Lepage (LF), the Kineras (KF) and the Foxville (FF). Geographical locations include Chapleau (C), Timmins (T), Kapuskasing (K), and Wawa (W). Modified from Percival and McGrath, (1986 p. 555).

or near the surface. These faults are believed to underlie the entire uplift and differences in the nature of exposures of the granulites along strike are interpreted to be due to variations of dip of the faults or depth of decollement (Percival and McGrath, 1986). Post-thrusting extension is interpreted to be responsible for the various normal faults that dissect the originally coherent thrust sheet into discrete tectonic blocks (Percival and McGrath, 1986).

### **Age of Uplift**

The age of uplift is still one the major unanswered questions concerning the evolution of the KSZ. Accurate dating is crucial in relating the history of this isolated feature to the other major structures of the Canadian shield.

The ages of supra-crustal sequences from the Abitibi and Michipicoten belts range between 2750 and 2700 Ma, establishing the earliest possible time of uplift (Percival and Card, 1983). Percival et al. (1988) suggest a minimum age for the uplift is constrained by the age of alkalic carbonatite complexes that intrude bounding faults of the structure; uplift must have preceded the oldest of these,

which is 1907 Ma.

Although the seismic data provide no direct evidence for the age of uplift, the geometries of the faults and the inferred shortening along these faults discussed in later chapters do have implication for timing. The arcuate 2.45 Ga Matachewan-Hearst dyke swarms cross the southern KSZ with only minor offsets in regions interpreted to be underlain by the major detachment. Unless the transport fortuitously followed the trend of the dykes, major horizontal movement must have preceded 2.45 Ga (Percival et al, 1989) or else the dykes would have been significantly offset.

### **Comparison with Rocky Mountain Structures**

Both Cook (1985) and Percival and McGrath (1986) draw similarities between the structures in the uplifted high grade rocks of the KSZ and the uplifted basement rocks of the Wyoming Province in the Rocky Mountains. Figure 2.3 is a schematic comparison between the interpreted cross-sectional geometries of both intracratonic uplifts. Although there are differences in terms of the scale and the arrangement of structures in map view, many similar styles of uplift and deformation have been interpreted to

exist in both regions, including thrust blocks, tilted thrust blocks and pop-up structures. The comparisons between the Wind River uplift (WR-WR') and the southern Chapleau block (C-C') and their associated thrusts are of particular interest here (Figure 2.3).

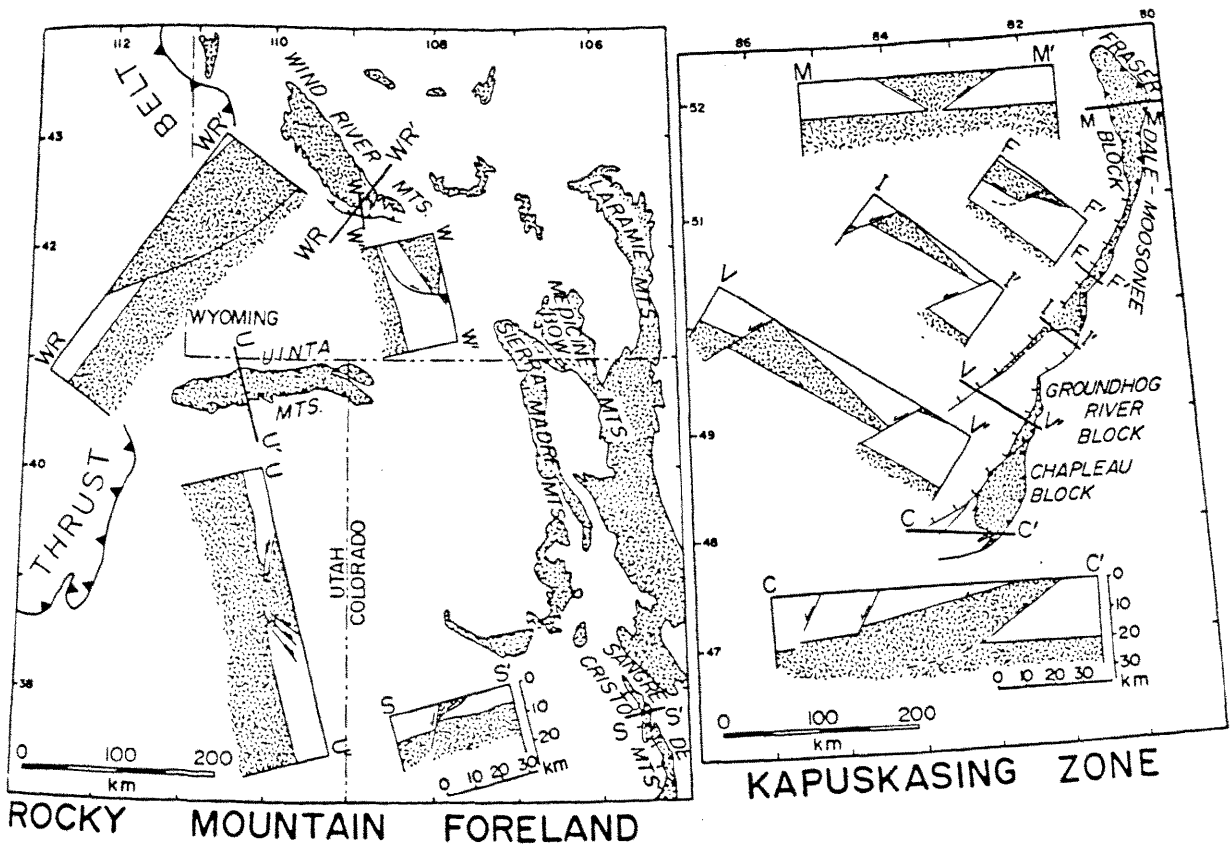


Figure 2.3: Maps and cross sections comparing structural configurations of individual components of the Kapuskasing structural zone and basement uplifts of the Rocky Mountains. Stipple pattern represents exposed Precambrian basement in the Rocky Mountains and greater than 6 kbar granulites in the KSZ. Of particular interest are the cross section WR-WR' from the Rocky Mountains and C-C' from the KSZ. (From Percival and McGrath, 1986; p. 567).

## CHAPTER-3: SEISMIC DATA BASE

### Seismic Data Acquisition

As part of the Phase-II LITHOPROBE Kapuskasing Structural Zone Transect, approximately 290 km of seismic reflection data were acquired over the Chapleau block between October, 1987 and January, 1988. Six profiles, lines 1-6, cross the southern end of the Chapleau block in several different directions allowing for regional 3-D coverage. Data were recorded (undershoots) to fill the gaps caused by inaccessible terrain between lines 2 and 3 and lines 3 and 4 with sources and receivers placed on opposite sides of gaps. All of these lines were recorded with conventional crustal reflection profiling parameters (Table 3.1). In addition line 2 was also recorded with high resolution parameters (Table 3.2). The purpose of recording the high resolution data in the Chapleau block was to provide the capability of correlating reflections with surface features as closely as possible particularly in the structurally complex area of the KSZ and ILFZ. The large bandwidth (20-130 Hz) also allows for high vertical resolution. For example, assuming  $1/4$  wavelength resolution, a velocity of 6000 m/s and a dominant frequency



**TABLE 3.1: REGIONAL DATA ACQUISITION PARAMETERS**

---

**SOURCE INFORMATION**

ENERGY SOURCE -	Four Mertz Model-18 vibrators
SWEEP SPECTRUM -	12 - 52 Hz (linear)
SWEEP LENGTH -	14 s
VERTICAL STACK -	8 times w/noise reject
VIBRATION INTERVAL -	100 m

**RECEIVER INFORMATION**

GEOPHONES -	Vertical motion sensitive
FIELD FILTERS -	Low-cut: out, anti-alias:in
LISTEN TIME -	18 s
UNCORRELATED RECORD -	32 s
CORRELATED RECORD -	18 s
SAMPLE RATE -	4 ms
GROUP INTERVAL -	50 m
CHANNELS -	240
COVERAGE -	60 fold
GROUP DESIGN -	12 geophones spaced over 50 m
SPREAD DESIGN -	Asymmetric split 60 stations north or west 13 station gap 180 stations south or east

---

**TABLE 3.2: HIGH RESOLUTION DATA ACQUISITION PARAMETERS**

---

**SOURCE INFORMATION**

ENERGY SOURCE -	Two Mertz Model-18 vibrators
SWEEP SPECTRUM -	20 - 130 Hz (linear)
SWEEP LENGTH -	8 s
VERTICAL STACK -	8 times w/noise reject
VIBRATION INTERVAL -	20 m

**RECEIVER INFORMATION**

GEOPHONES -	Vertical and in-line horizontal motion sensitive
FIELD FILTERS -	low-cut: out, anti-alias:in
LISTEN TIME -	8 s
UNCORRELATED RECORD -	16 s
CORRELATED RECORD -	8
SAMPLE RATE -	2 ms
GROUP INTERVAL -	20 m
CHANNELS -	120
COVERAGE -	60 fold
GROUP DESIGN -	12 geophones spaced over 25 m for vertical, 2 geophones over 12 m for horizontal
SPREAD DESIGN -	End on, 8 station gap Source on west end

---

of 50-60 Hz will allow vertical resolution of 20-25 m layers.

### **Seismic Data Processing**

The initial seismic data processing was contracted to Veritas Seismic of Calgary. The data were processed through a standard common mid-point (CMP) processing sequence with all parameters chosen by myself and other researchers involved in the LITHOPROBE Kapuskasing project. Tables 3.3 and 3.4 summarize these parameters. Additional post stack processing was done at the Lithoprobe Seismic Processing Facility (LSPF) at The University of Calgary using CogniSeis DISCO software.

### Coherency Filtering

When seismic data have a low signal to noise ratio (S/N), as crustal seismic data often do, it is useful to extract the coherent portion of the data by using some type of automated statistical process. By filtering random noise from seismic data, geometric relationships are more readily observed and are easier to interpret.

**TABLE 3.3: REGIONAL PROFILE PROCESSING PARAMETERS**


---

DEMULTIPLEX

ADJACENT RECORD SUMMATION

AMPLITUDE RECOVERY - 2000 ms AGC

GEOMETRY - Crooked Line

ELEVATION STATICS - Datum - 400 m A.S.L.  
Replacement Velocity - 5000 m/s

CMP GATHER - Approx. 35 Fold

VELOCITY ANALYSIS

NORMAL MOVEOUT CORRECTION

FIRST BREAK MUTES

TRIM STATICS - Variable Correlation Window

STACK - Approx. 35 fold

BANDPASS FILTER - 8/12 - 52/62  
Gate: 0 - 16000 ms

AMPLITUDE EQUALIZATION - Time Variant Mean

TRACE MIX - 3 Trace  
Weight: 25% - 50% - 25%

MIGRATION

---

**TABLE 3.4: HIGH RESOLUTION PROFILE PROCESSING PARAMETERS**


---

 DEMULTIPLEX

AMPLITUDE RECOVERY - 2000 ms AGC

GEOMETRY - Crooked Line

 ELEVATION STATICS - Datum - 400 m A.S.L.  
 Replacement Velocity - 5000 m/s

CMP GATHER - 64 Fold (max.)

## VELOCITY ANALYSIS

## NORMAL MOVEOUT CORRECTION

## FIRST BREAK MUTES

 TRIM STATICS - Correlation Window:  
 400 - 6000 ms

STACK - 64 Fold (max.)

 BANDPASS FILTER - V.P. 101-524:  
 15/20-110/120 Gate 0-4000 ms  
 15/20-100/110 Gate 4000-8000 ms

 V.P. 525-1031:  
 15/20-120/130 Gate 0-4000 ms  
 15/20-100/110 Gate 4000-8000 ms

AMPLITUDE EQUALIZATION - Time Variant Mean

 MIGRATION
 

---

Two program modules, SIGNAL and DIGISTK, which perform such coherency filtering are available in the DISCO software package. The first module, SIGNAL, extracts the coherent signal of the data. The second module, DIGISTK, allows the original data to be mixed back with a weighted amount of the determined signal. The SIGNAL algorithm is similar to most coherency filtering techniques (e.g. Neidell and Taner, 1971; Kong et al, 1985; Milkereit and Spencer, 1988), where the data are scanned over a range of dips, searching for a preset coherency or semblance threshold. If this threshold is not met, the data are either attenuated by some amount or rejected entirely. In the SIGNAL algorithm, higher threshold values allow for more noise rejection. This whole procedure is applied over a series of moving trace windows (array widths) in both distance and time.

Two primary considerations were used in the SIGNAL parameter selection. The first was to produce a filtered section that displayed a minimum amount of background noise, without removing any geometric information. As the SIGNAL process is computationally intensive, the second consideration is practical and involved selecting parameters that minimized the run time of the process. The array width and threshold value are parameters that have the most significant affect on the noise rejection. As a rule of thumb, large array widths (e.g. 21 traces or more)

with a lower threshold value (e.g. 0.20) produce similar results to small array (e.g. 15 traces) with a larger threshold (e.g. 0.35). The parameters that most significantly affect the run time are the increments for the both the distance and time windows. The larger the increment, the less time it takes to run the process.

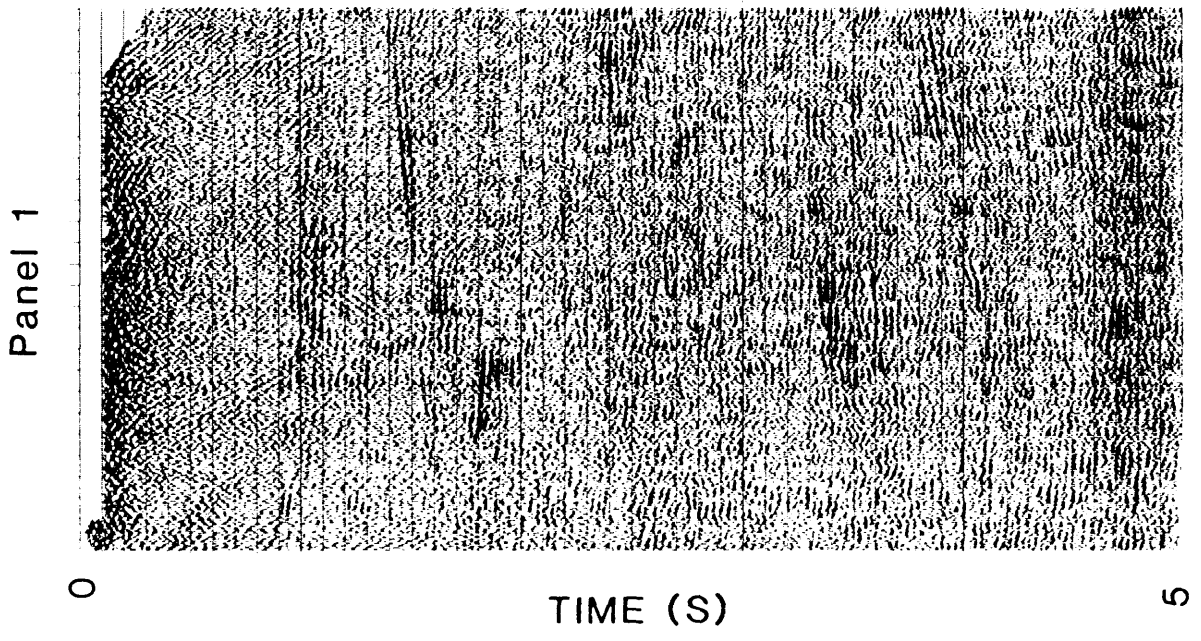
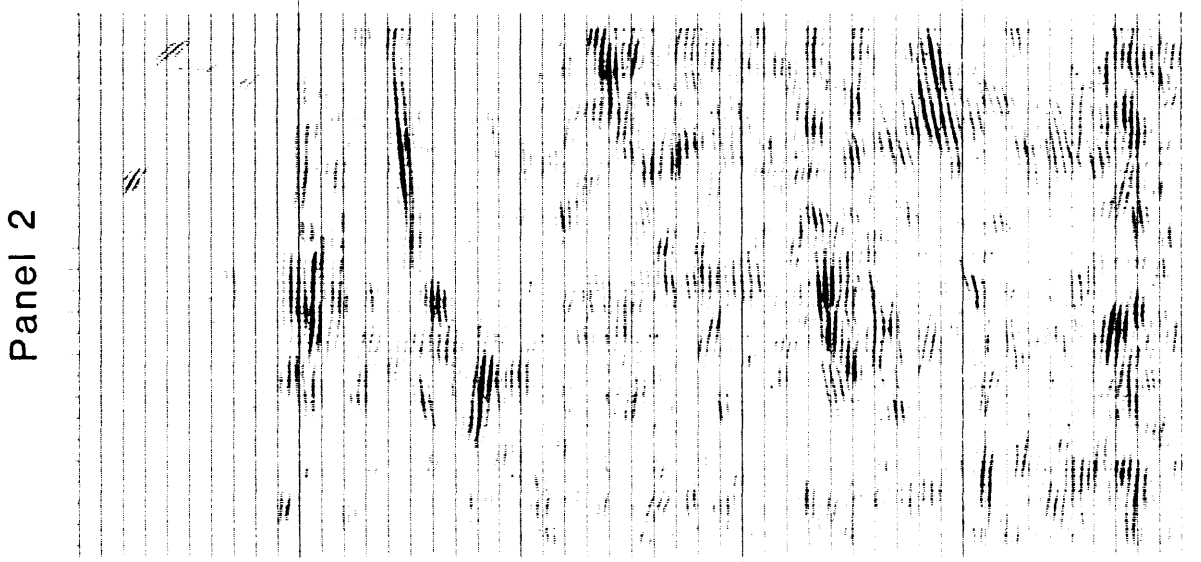
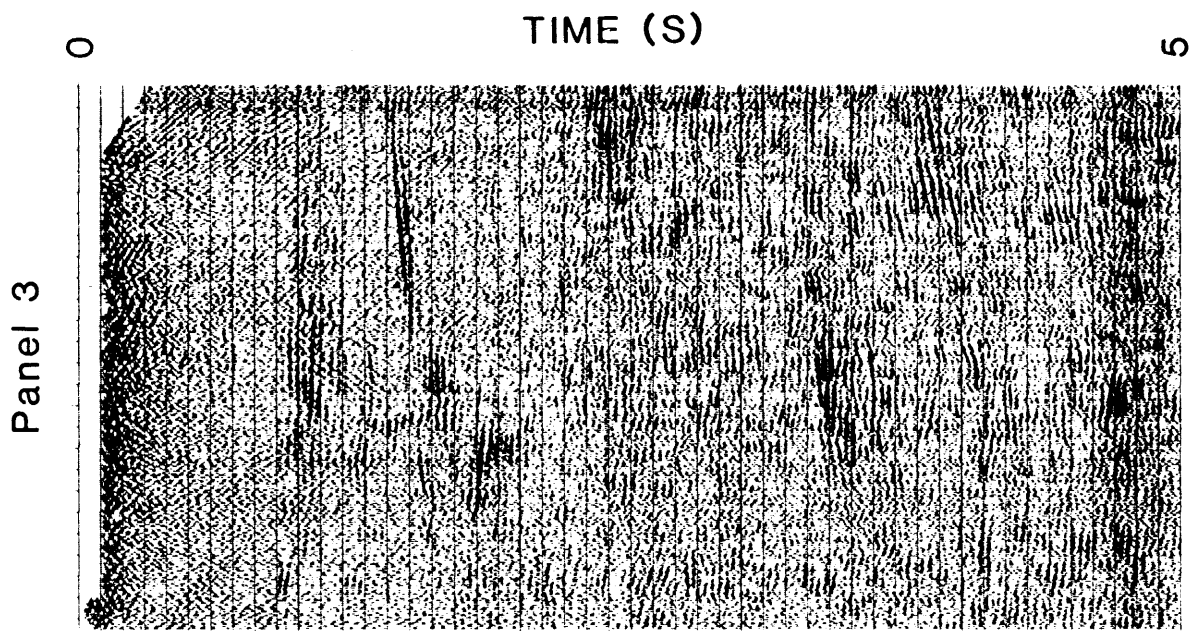
An example of the results of applying this procedure to a portion of Kapuskasing line 3 is shown in Figure 3.1. Panel 1 displays the original unfiltered data. These data have been processed through the conventional processing flow by the contractor (Table 3.3). Panel 2 is the coherent signal extracted from the data using the SIGNAL algorithm. For this run, a 17 trace distance window that was incremented by 3 traces after each complete set of scans in time was used. The data were scanned over an 80 ms time window (incremented by 32 ms) between dips ranging from -200 to 200 ms/array width (incremented by 20 ms/array width). The coherency threshold was set at 0.25. Panel 3 displays the data with a 50/50 mix of both the original and the signal extracted data.

Coherency filtering is largely a cosmetic process and can be loosely thought of as an automated line diagram generator. It has clarified the geometric relationships between reflections on the data, allowing easier structural interpretation. Coherency filtered sections are also more amenable to photographic reduction as they have less

background noise. Sections that have had a light (25%) mixing of the coherent signal with the original data using the DIGISTK module have been easier to interpret on the Landmark Graphics Workstation. After the DIGISTK process, reflections become more prominent but the data still have the necessary contrast in amplitude for display on the workstation monitor.



Figure 3.1: (next page) Example of coherency filtering process. Panel 1: original data from line 3, Panel 2: extracted signal, Panel 3: a 50%/50% mix of original data and signal.



## CHAPTER 4: REPROCESSING OF REGIONAL LINE 2

### Introduction

Initial processing of regional seismic line 2 produced a stacked section that was surprisingly different than the high resolution profile recorded along the same line. Figures 4.1 and 4.2 compare the original processing between the two data sets. Some of the structures crucial to the interpretation, which are imaged on the high resolution data, are poorly resolved or absent on the regional data. For example reflections labeled A are only partially imaged on the regional data and reflections B and C are not seen on the east end of the regional profile at all (Figure 4.1 and 4.2). These results produced some concern as they suggested that a considerable amount of information was not being recorded with the regional data, or was being overlooked in the initial processing.

The purpose of this chapter is to examine these differences by additional careful prestack processing of regional line 2 and to determine how an improved image can be obtained from the regional data. The processing techniques used are standard; hence they are not discussed in detail (see Yilmaz, 1987 for a discussion on seismic

Figure 4.1: (next page) Original processing of line 2 regional with the prestack summation of adjacent shot gathers. See Table 3.3 for parameters.

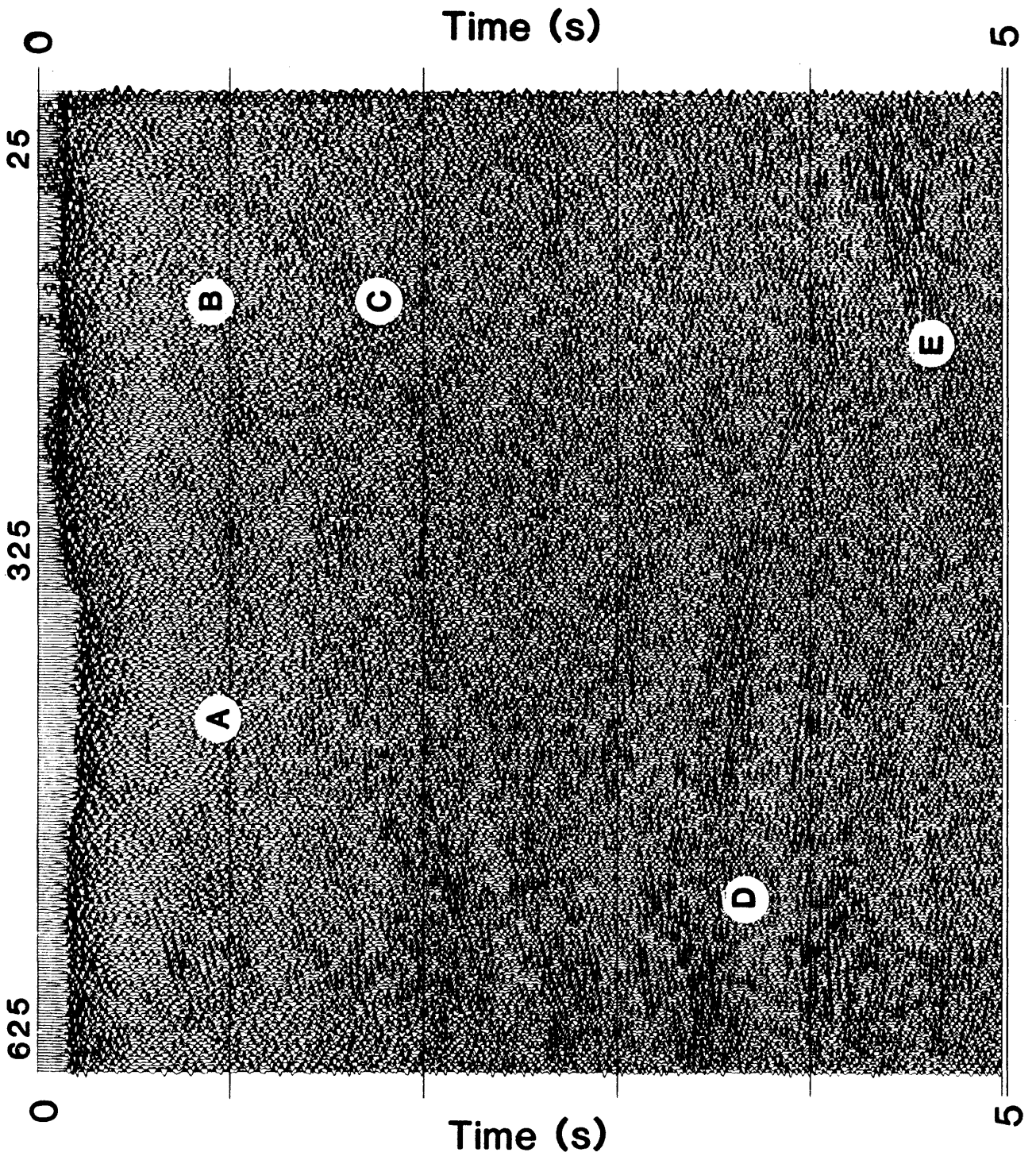
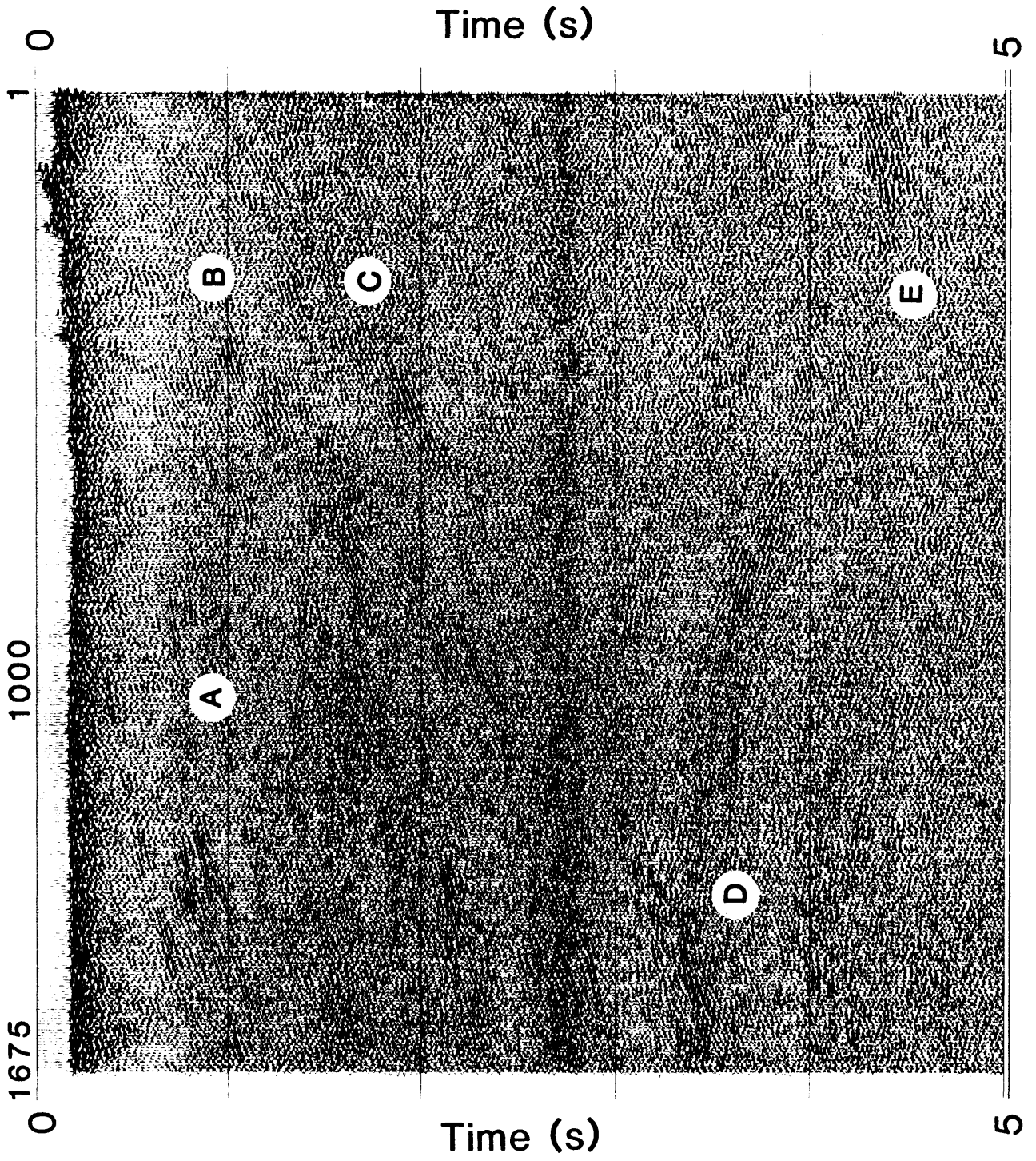


Figure 4.2: (Next page) Original processing of line 2 high resolution. See Table 3.4 for parameters.



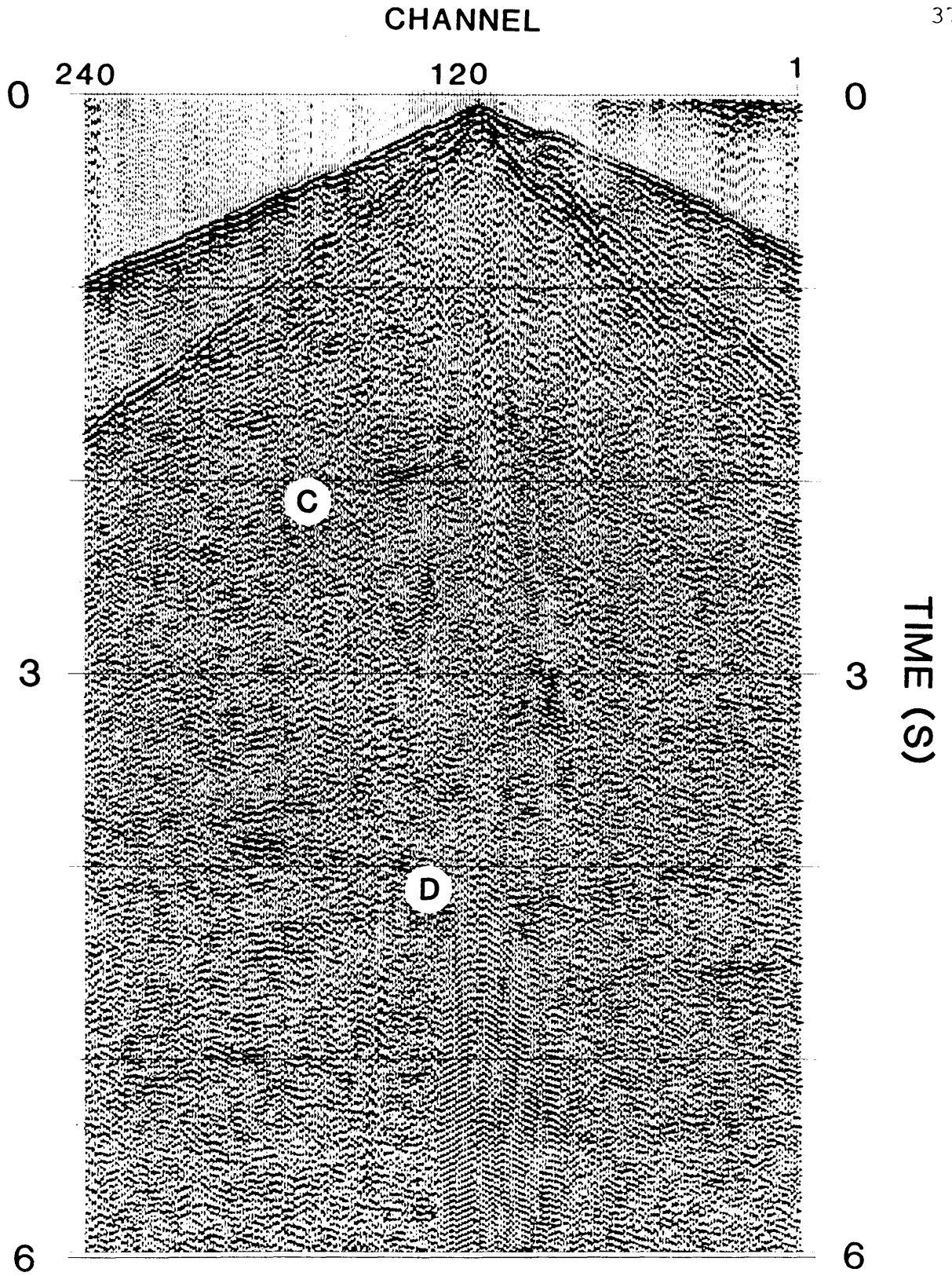
data processing). However, considerably more effort was expended on parameter choices to enhance detail, and to produce a section from the regional data that closely approximated a band limited version of the higher resolution data set.

### **Standard Reprocessing Comparison**

In order to reduce the amount of data processed in the original contract, adjacent shot gathers from the regional profiles were summed prior to the initial CMP processing. It was assumed that a summation of adjacent shot gathers would have approximated a group interval of 100 m and V.P. interval of 200 m, which was typical of earlier LITHOPROBE surveys. It was first suspected that such summing degraded the imaging quality, and could thus account for the differences between the high resolution and regional sections. For example, Figures 4.3 and 4.4 show two adjacent shot gathers (V.P.'s 189 and 191) from regional line 2 and shown in Figure 4.5 is the result of their summation. Several events have been labeled: event C is a west dipping reflection corresponding to reflection C on the stacked data and event D corresponds to the arcuate event on the stacked data. After summation, due to the

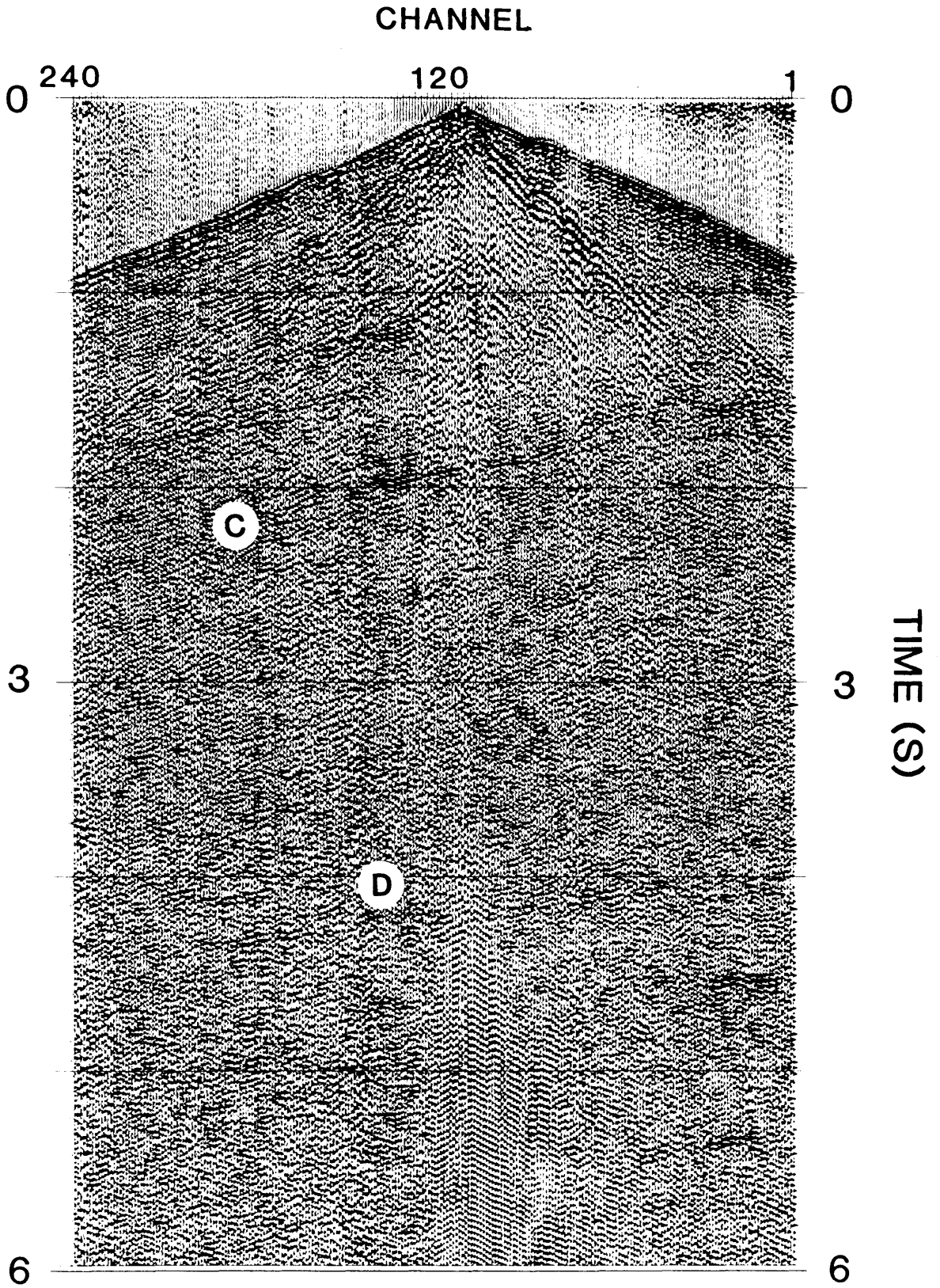


Figure 4.3: (next page) Shot gather from V.P. 189



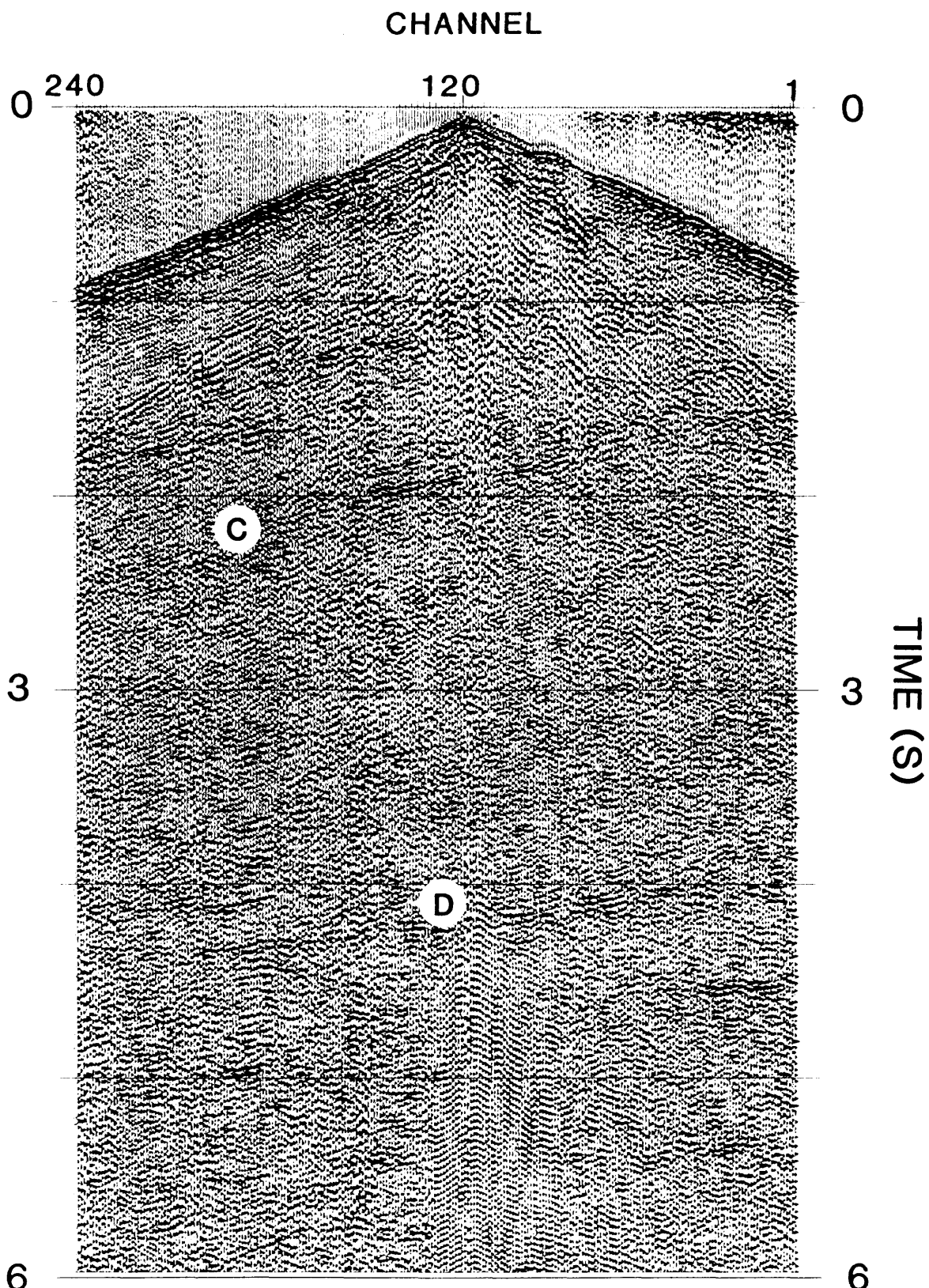
Shot gather from V.P. 189

Figure 4.4: (next page) Shot gather from V.P. 191



Shot gather from V.P. 191

Figure 4.5 (next page) Summation of shot gathers from V.P.'s 189 and 191.



Summation of shot gathers

reduction of random noise caused by the stacking of the two records, the data have a better (not worse) appearance.

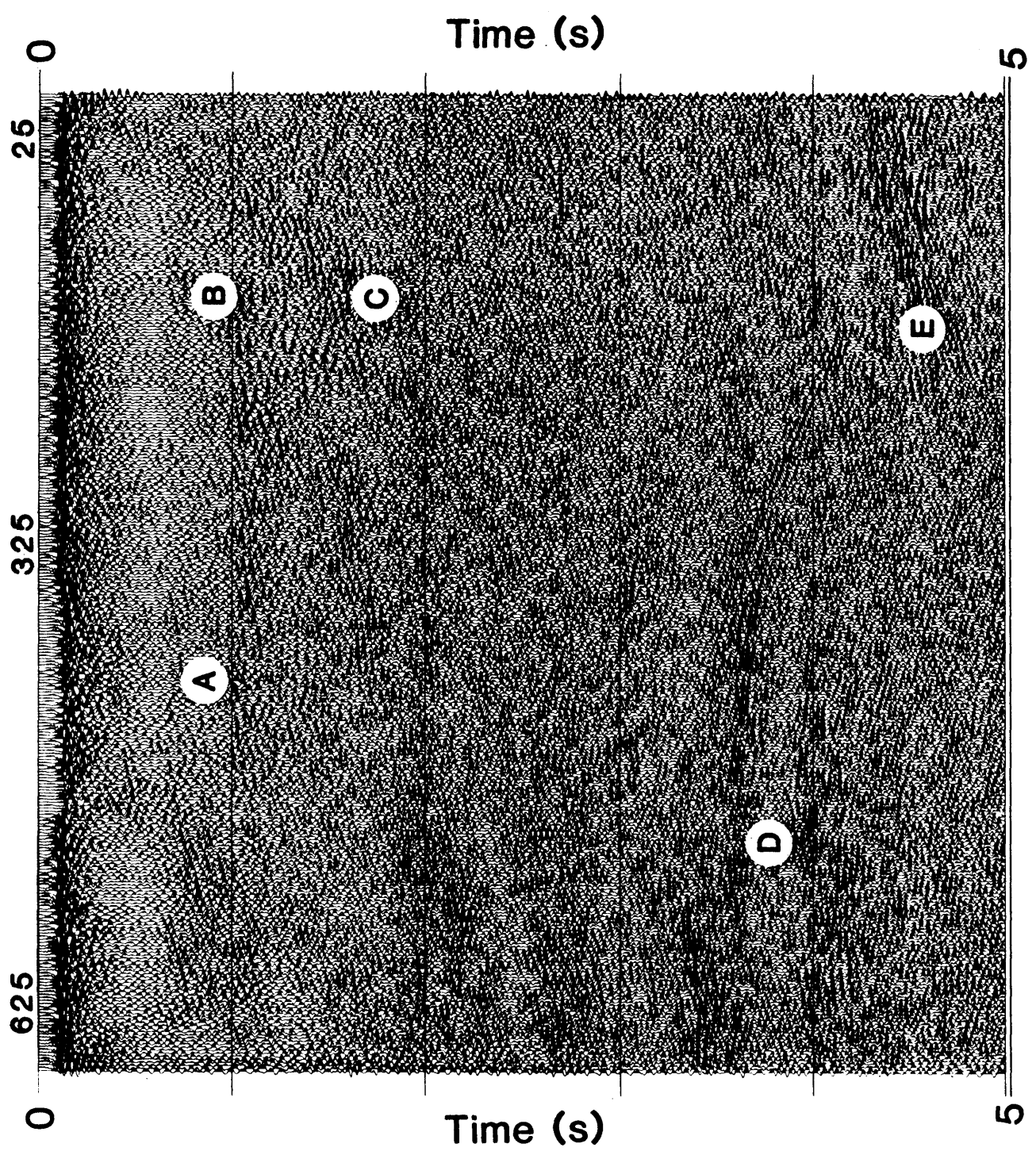
In order to examine the effect of no record summation on the stacked data, the regional data without the prestack summation of shot gathers was then reprocessed using a sequence that followed the original processing flow (Table 3.3) implemented on CogniSeis DISCO software at the LSPF. However, it should be noted that a slightly different first break mute pattern was used in the reprocessing. As the reprocessing results only show marginal improvement in coherency and amplitude of reflections, (most noticeable in the reflections below 3.0 s) as compared to the original regional section (Figures 4.1 and 4.6), it is apparent that the prestack summation cannot account for the major differences between the regional and high resolution sections.

### **Additional Signal Enhancement**

Although there is some very limited improvement over the original regional section when processed without the shot gather summation, the quality of the regional data is still substantially inferior to that of the high resolution data. Accordingly, attempts were made to produce a section from

Figure 4.6: (Next page) Identical reprocessing without prestack summation of shot gathers.





the regional data that is comparable to the high resolution data using careful application of standard signal enhancement techniques. During the initial processing of the regional and high resolution data sets, several parameters used in the construction of a stacked sections had different values. Thus, in order to do a fair comparison, the data sets were filtered to a common bandwidth (20-55 Hz) and parameters similar to those used in the original processing of the high resolution data were applied to the regional data and include: 1) applying similar stacking velocity functions, 2) using similar offset ranges, and 3) using a similar correlation statics window.

Shown in Figure 4.7 are the high resolution data bandlimited using a tapered boxcar filter with a 20 Hz low cut, a 25 Hz low pass, a 45 Hz high pass, and 55 Hz high cut design. Shown in Figure 4.8 are the reprocessed regional data with the same filter applied. Although some improvement is seen in the regional data due to the filtering of the low frequency surface wave and other noise, there are still some significant differences between the two data sets. The coherency of reflections A, B and C is still better on the bandlimited high resolution data.

The next major difference between the two data sets that was investigated was the offset range used in the stacking process. Offset range can have a significant effect on the

Figure 4.7: (next page) Line 2 high resolution bandlimited to 20/25/45/55 Hz.

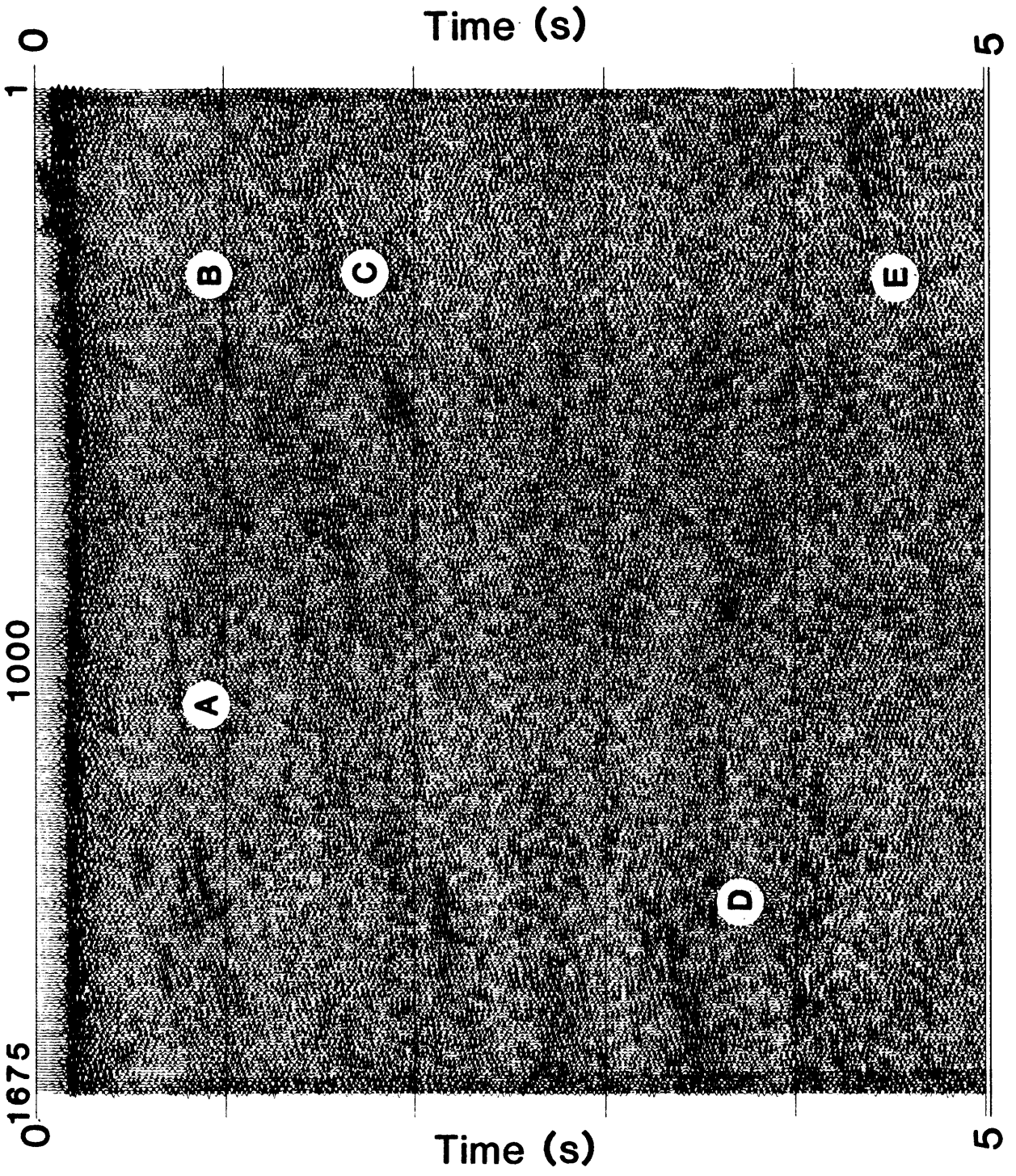
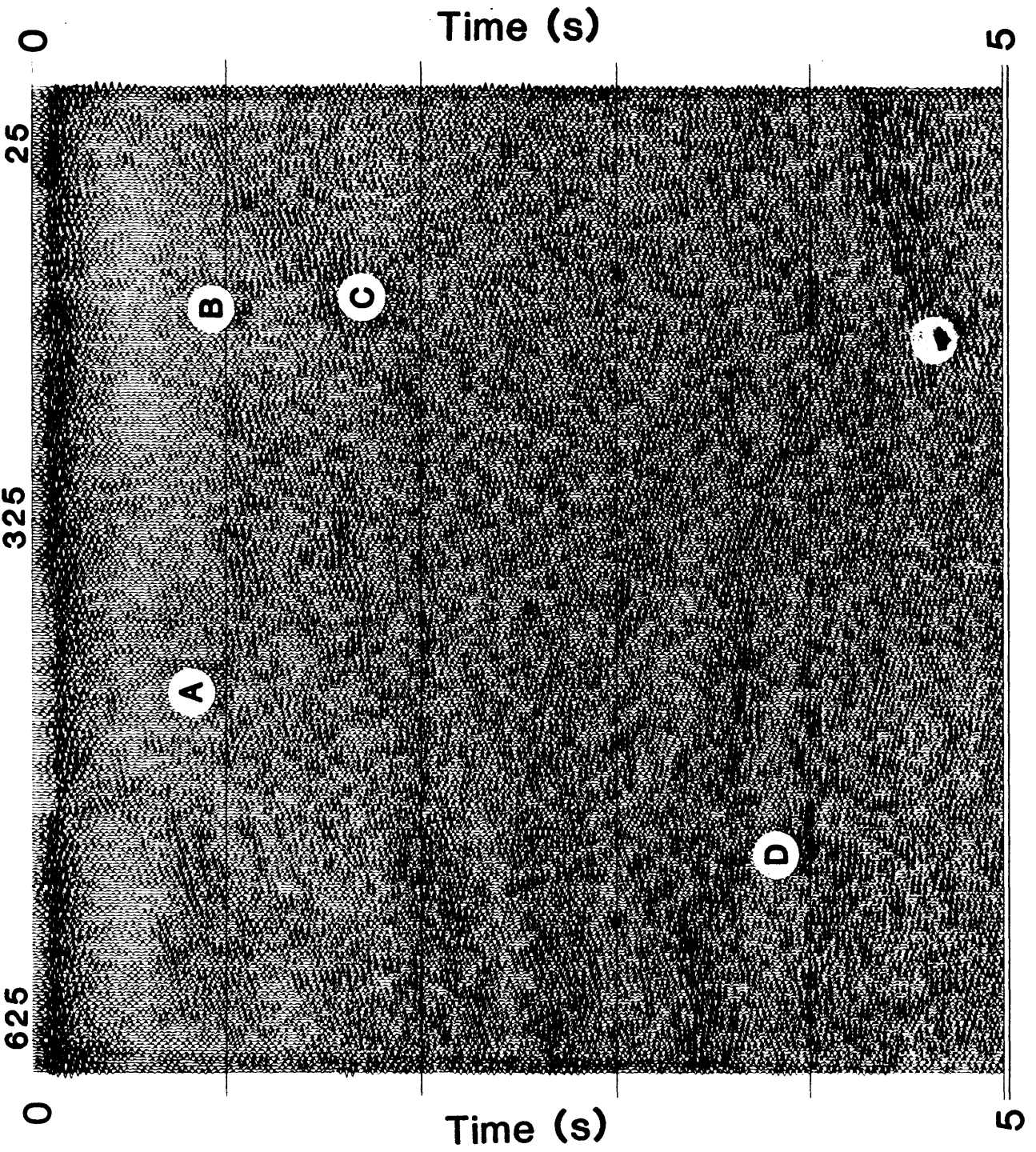


Figure 4.8: (next page) Reprocessed line 2 regional (Figure 4.6) band limited to 20/25/45/55 Hz.



quality of the stack section, particularly when the offset is very large compared to the depth of the reflector. This condition violates the assumption of near vertical incidence of raypaths used in conventional move out corrections. The maximum offset used in the high resolution survey was about 2.5 km, whereas when rolling into the spread, offsets up to 12.0 km were used in the regional acquisition. Thus, to further facilitate comparison of the two sections the regional data were limited to offsets of 2.5 km or less.

The final major difference between the original processing of the high resolution data and the regional data was the time window used in correlation statics. Correlation statics is a method that corrects for minor static shifts between traces within normal move out corrected CMP gathers based upon a statistical cross correlation function (Taner et al, 1974). Each trace within a CMP gather is cross-correlated over a specified time window with its corresponding stacked trace and is then adjusted in time to a position where the correlation is the highest. Subsequently, each CMP gather is restacked, yielding events with improved amplitude and coherence. The original correlation window on the high resolution data was 400 to 6000 ms, whereas a 1000 to 6000 ms window was used in the original processing of the regional data. Since many reflections can be traced up to

about 300 ms on the high resolution data, using a correlation window for the regional data that encompasses the early times should improve the coherence of these shallow events.

Figure 4.9 shows the regional section processed with frequency, offset, velocity and correlation statics parameters that are comparable to the band limited high resolution section (Figure 4.7). The quality of the regional section is now nearly equivalent to the high resolution section; in some regions it has actually imaged structures better. Events A, B and C, are now clearly visible on the regional data, and events D and E (all events discussed in Chapter 5) are more coherent and have a higher relative amplitude on the regional data (probably due to the greater amount of input energy with more vibrators - Table 3.1). However, the regional data still appear to have a slightly lower frequency content than the high resolution data, even though both data sets are bandpass filtered to the same frequency range.

Figure 4.10 compares the amplitude spectra from portions of the two data sets. The spectra from the high resolution data show only a slight decay of amplitude in the upper end of the frequency band, whereas the spectra from the regional data show a more pronounced decay of the higher frequencies. This observation is puzzling and no definite explanation for the difference can be offered. However,



Figure 4.9: (next page) Line-2 regional reprocessed with parameters that are comparable to a bandlimited version of line 2 high resolution (Figure 4.7).

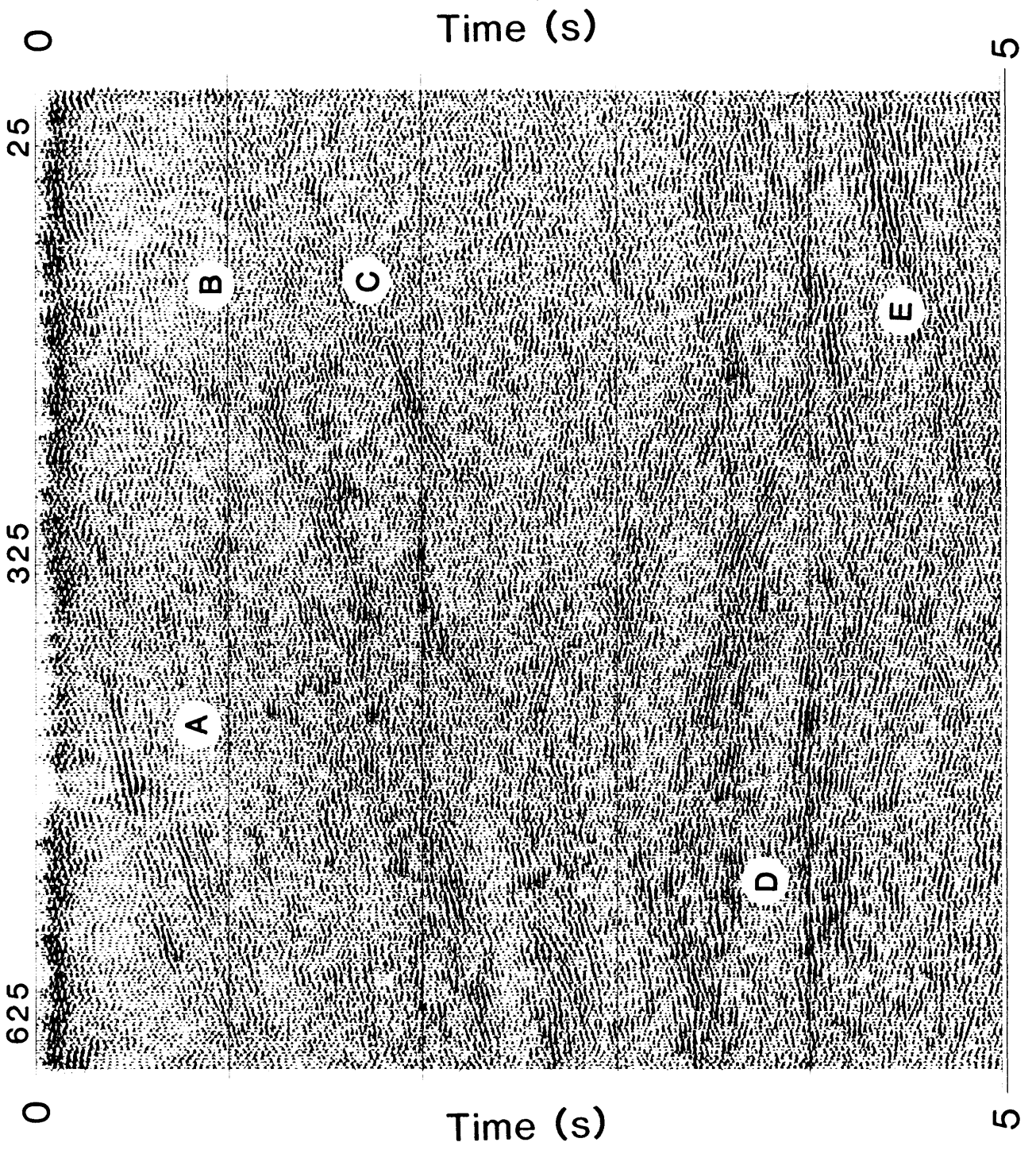
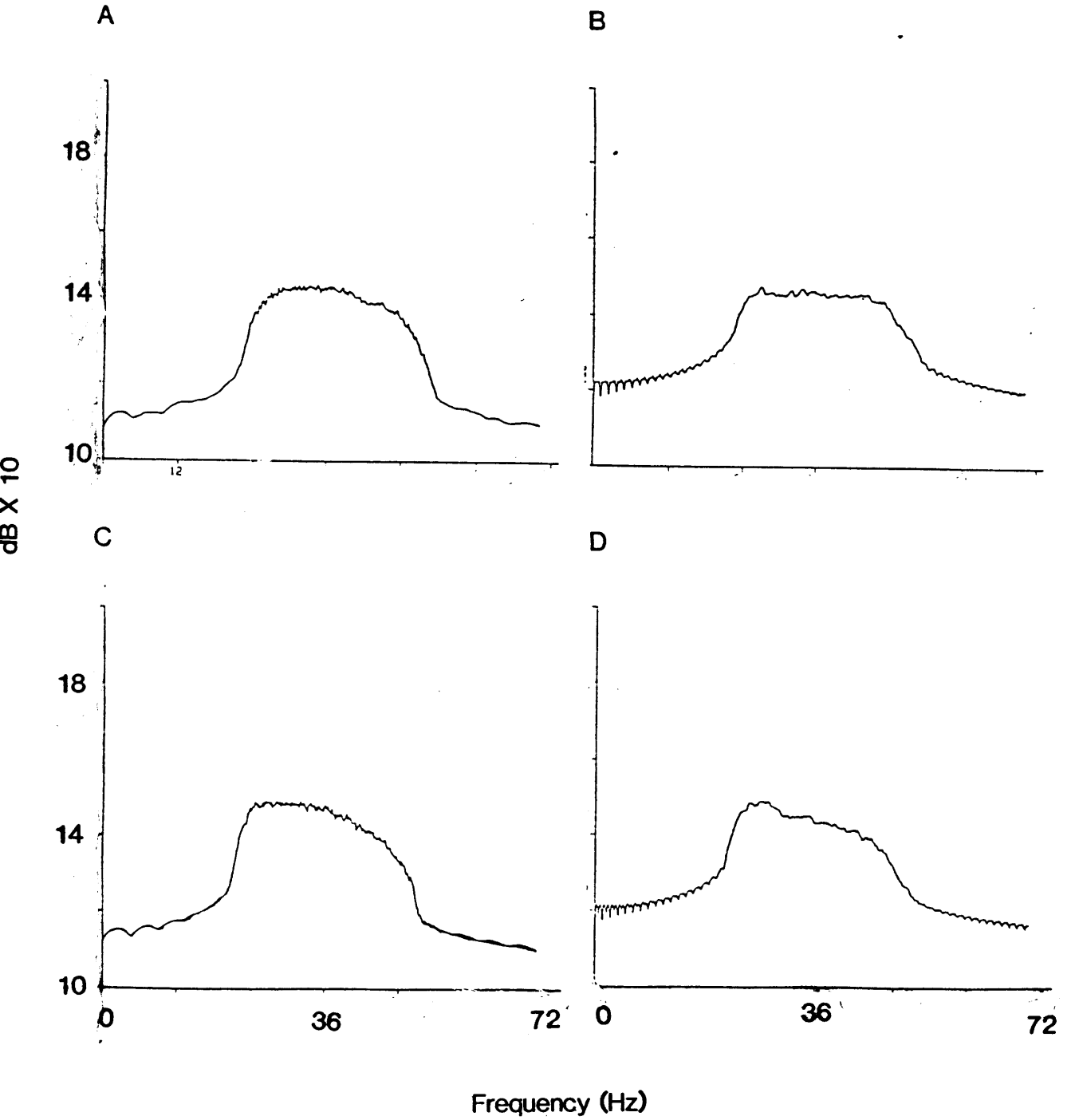
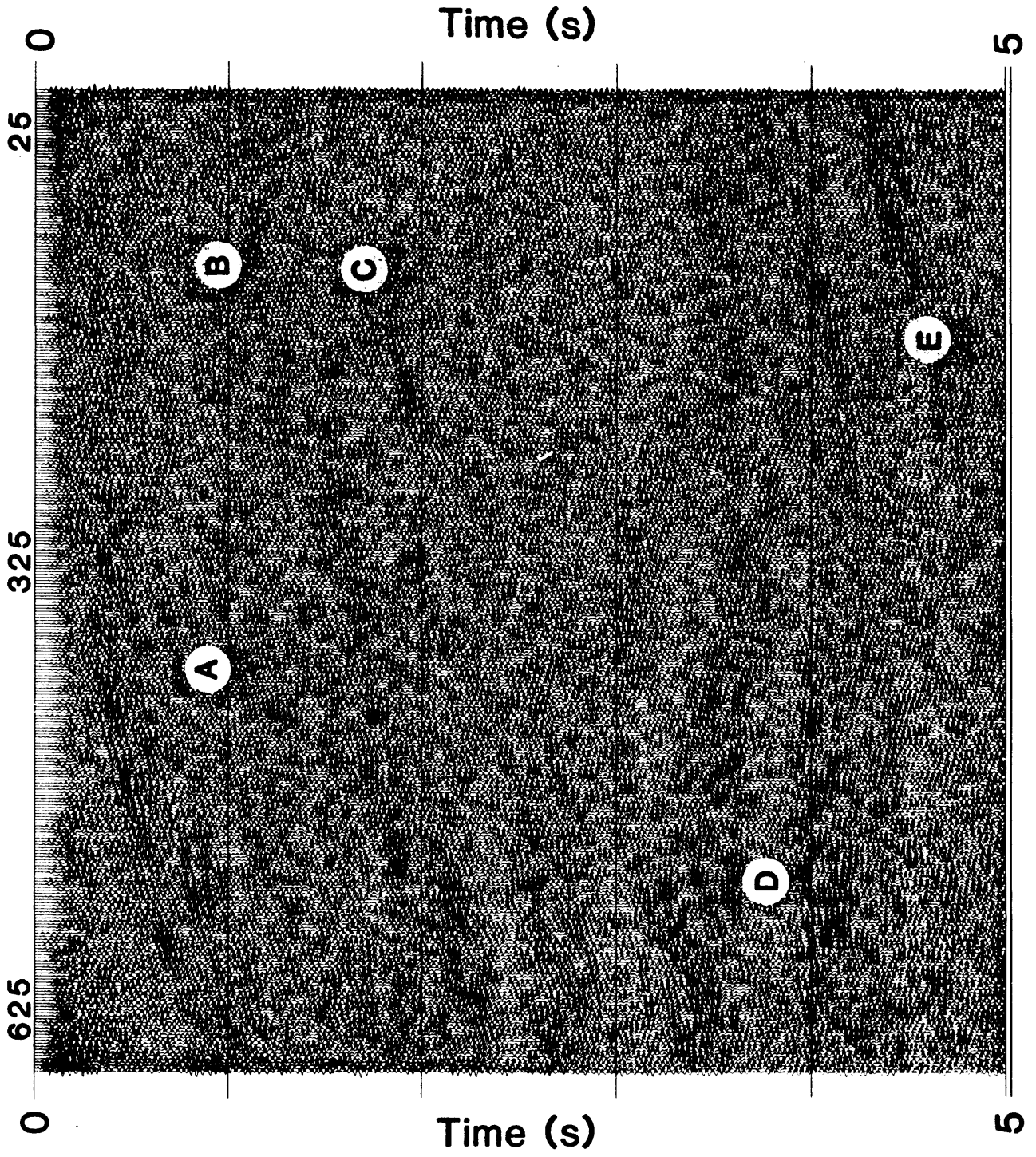


Figure 4.10: (next page) Comparison of mean amplitude spectra from bandlimited versions of the regional and high resolution data. A) Spectrum from high resolution data between CDP's 21-601 and time window of 500-4500 ms. B) Spectrum from high resolution data between CDP'S 1001-1601 and a time window of 300-1100 ms. C) Spectrum from regional data between CDP's 25-275 and a time window of 500-4500 ms. D) Spectrum from regional data between CDP's 375-625 and a time window of 300-1100 ms.



two possibilities include: 1) different coupling effects or ground conditions during acquisition, causing slight attenuation of the higher frequencies, and 2) greater effort (time) spent in the lower frequencies by the vibrators during the recording the regional data. Nevertheless, as the regional input energy ranged from 8-52 Hz, the amplitude of the higher frequencies can be balanced relative to the lower frequencies using spectral balancing techniques. Spectral balancing effectively enhances or increases the amplitude of specified frequencies, compensating for frequency loss with propagation of the seismic wave. Figure 4.11 shows the reprocessed regional section with parameters comparable to the high resolution section and a prestack spectral balance. Comparison of the section with the bandlimited high resolution section (Figure 4.7) now shows that both data sets appear to have the same frequency appearance, and comparison of Figures 4.10 and 4.12 shows that indeed the amplitude spectra are similar.

Figure 4.11: (next page) Reprocessed version of line 2 regional (Figure 4.9) with prestack spectral enhancement.



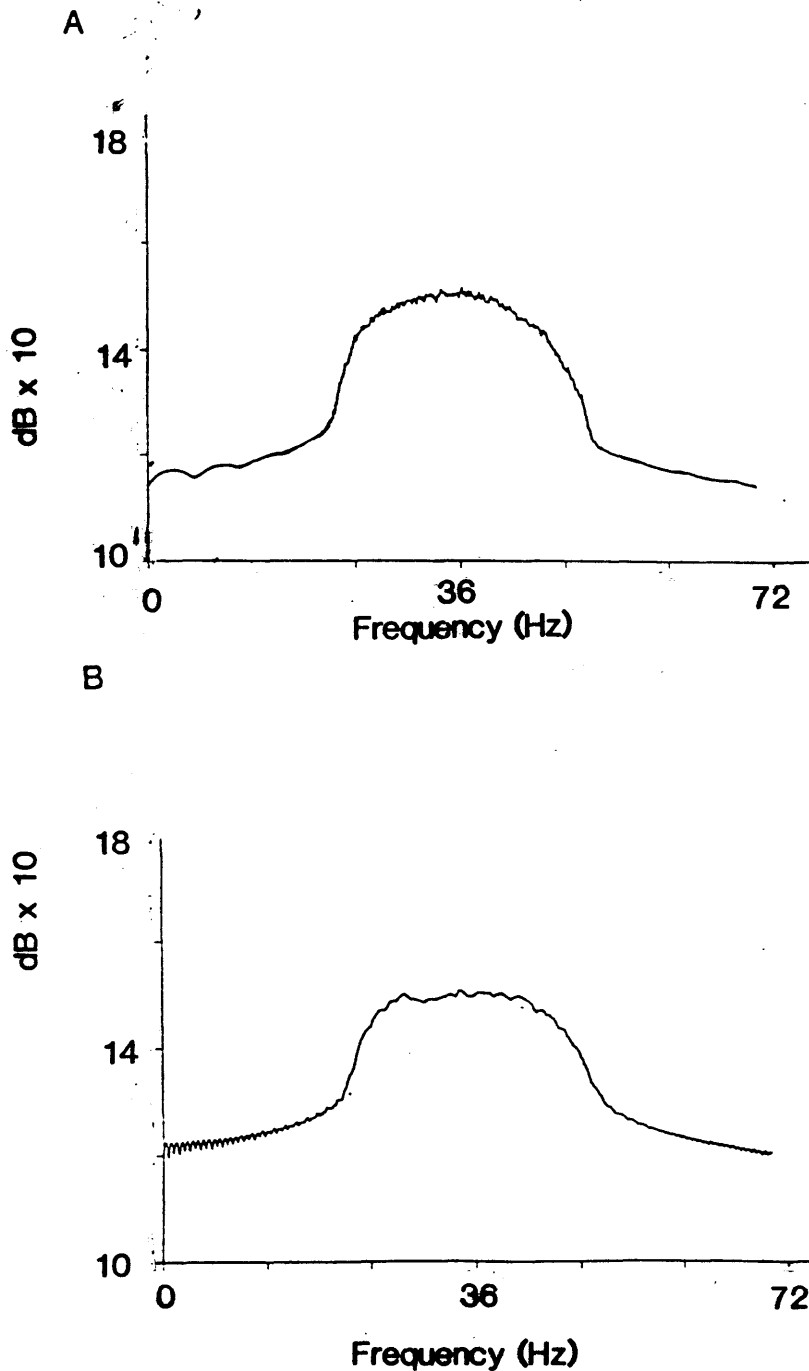


Figure 4.12: Amplitude spectra from same portions of the regional data shown in Figure 4.10 after spectral enhancement. A) CDP's 25-275 between 500-4500 ms. B) CDP's 375-625 between 300-1100 ms.



## Summary of Chapter 4

The initial processing of line 2 showed that the imaging using the regional parameters was substantially inferior to that of the data acquired with high resolution parameters. It was originally suspected that a prestack summation of adjacent shot gathers in the regional data processing could account for the difference. However, using conventional reprocessing techniques it was found that the summation of shot gathers could only account for very minor difference between the two sections. Reprocessing with carefully selected parameters, however, showed that the most important considerations for enhancement of the regional data are the offset range used in the CMP stacking process and the time window used in correlation statics. Using a short offset range (2.5 km or less) and a correlation statics window that encompasses early times, produces a section from the regional data that is nearly identical to a version of the high resolution data filtered to the same frequency range. Additional improvement can be obtained by applying a prestack spectral balance to compensate for frequency variation in the regional data.

The results from reprocessing the regional data are very important not only for the reprocessing of the Kapuskasing data set, but also for any future LITHOPROBE surveys. As

an image comparable to a bandlimited version of the high resolution data can be obtained from regional line 2, careful reprocessing will likely improve the images from the remaining regional profiles in the Kapuskasing survey. High resolution surveys can cost considerably more than regional surveys and if a good quality image can be produced by processing the regional data with emphasis placed on the shallow portion of the section, the recording of high resolution data may, in some areas, be unnecessary. In future LITHOPROBE transects two processing flows may be appropriate. The first would concentrate on the deeper reflections in which all of the offsets would be used in order to obtain maximum noise reduction in the stacking process, and the second would follow a sequence that concentrates on the shallow reflections.

## **CHAPTER 5: THIN THRUST SHEET FORMATION OF THE KSZ**

### **Introduction**

In this chapter the seismic reflection geometry along the east-west traverse (Lines 2, 3 and 4; Fig. 1.1) will be described in an effort to produce a regional cross section across the Chapleau block. The high resolution data along line 2 provide the best tie to the surface geology and therefore constrain the interpretation with the known location of the ILFZ. The east-west data provide the evidence for a ramp and flat style of thin thrust sheet(s) in the KSZ.

### **Local Geology Along the Seismic Profiles**

The east-west seismic transect (Figure 1.1) begins in the east at the ILFZ, crosses the Chapleau block and terminates in the west in the Wawa gneiss terrane. The surface geology along this transect comprises a wide variety of rock types including mylonite, granite, mafic gneiss, paragneiss, tonalitic gneiss and gabbroic

anorthosite.

In the vicinity of the eastern end of line 2, the ILFZ is bordered by two principal faults that define a zone of brittle and ductile deformation (Figure 5.1). Exposures at the eastern end of the profile are granodiorite, resembling rocks of the Abitibi subprovince, but separated from them by the easternmost bounding fault of the ILFZ. The westernmost fault bounding the ILFZ juxtaposes the gently northwest dipping sequence of high grade tonalitic, mafic and metasedimentary gneisses of the KSZ against the granodiorite. About 15 km to the south, Bursnall (1989) has mapped a 50-70 m wide mylonite zone associated with the ILFZ.

Towards the west, along lines 2 and 3, isolated within the high-grade gneisses, is the Shawmere anorthosite complex which is composed of massive to moderately foliated calcic anorthosite, gabbro and peridotite (Simmons et al. 1980; Riccio, 1981). Further to the west along line 4, the KSZ grades into the lower-grade tonalitic rocks of the Wawa gneiss terrane (Percival and Fountain, 1989; Moser, 1989). The Wawa gneiss terrane is characterized by tonalitic rocks with subhorizontal to domal high-strain zones, including the Robson Lake dome (Moser, 1989), an inlier of high grade Kapuskasing gneisses.

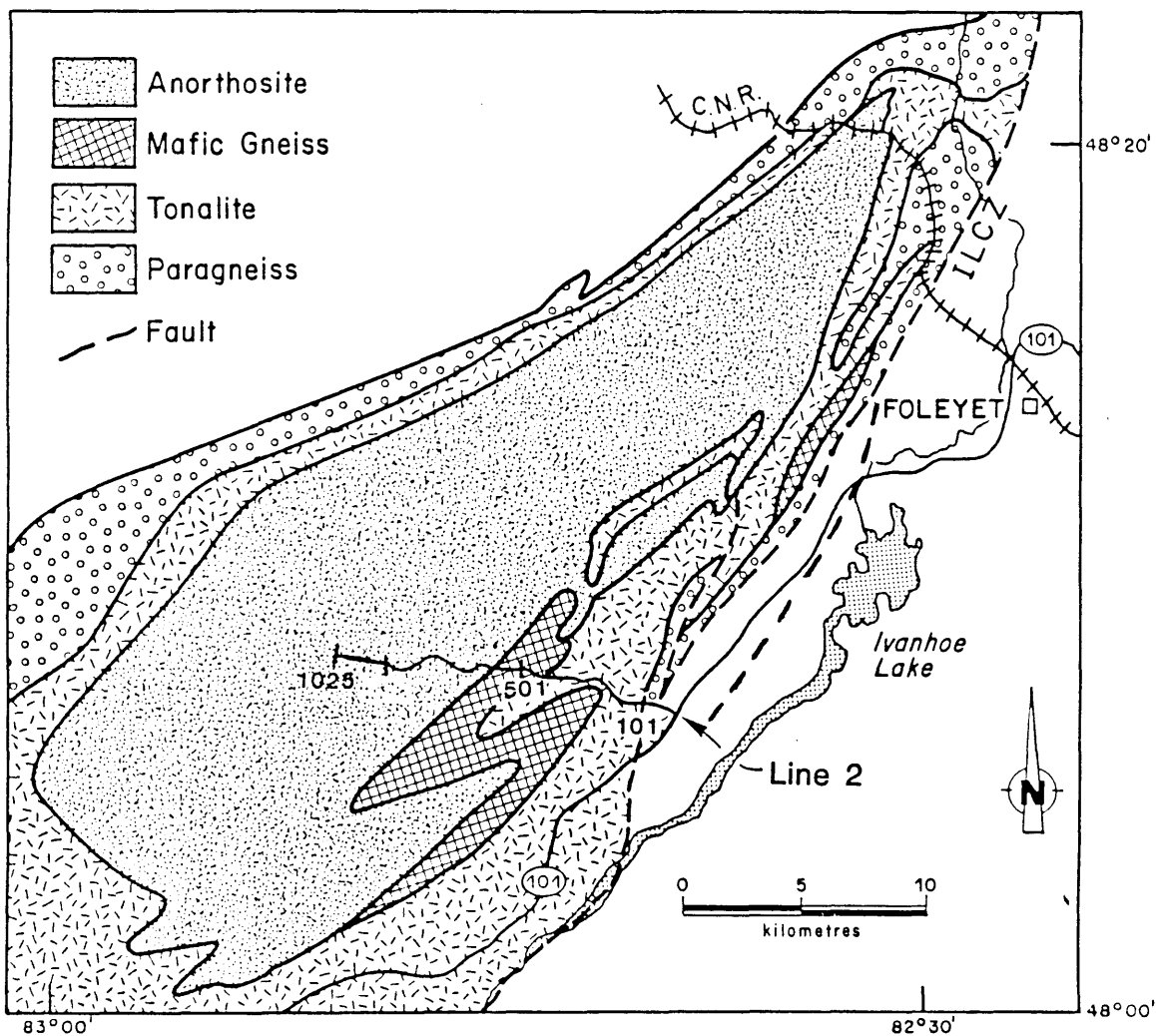


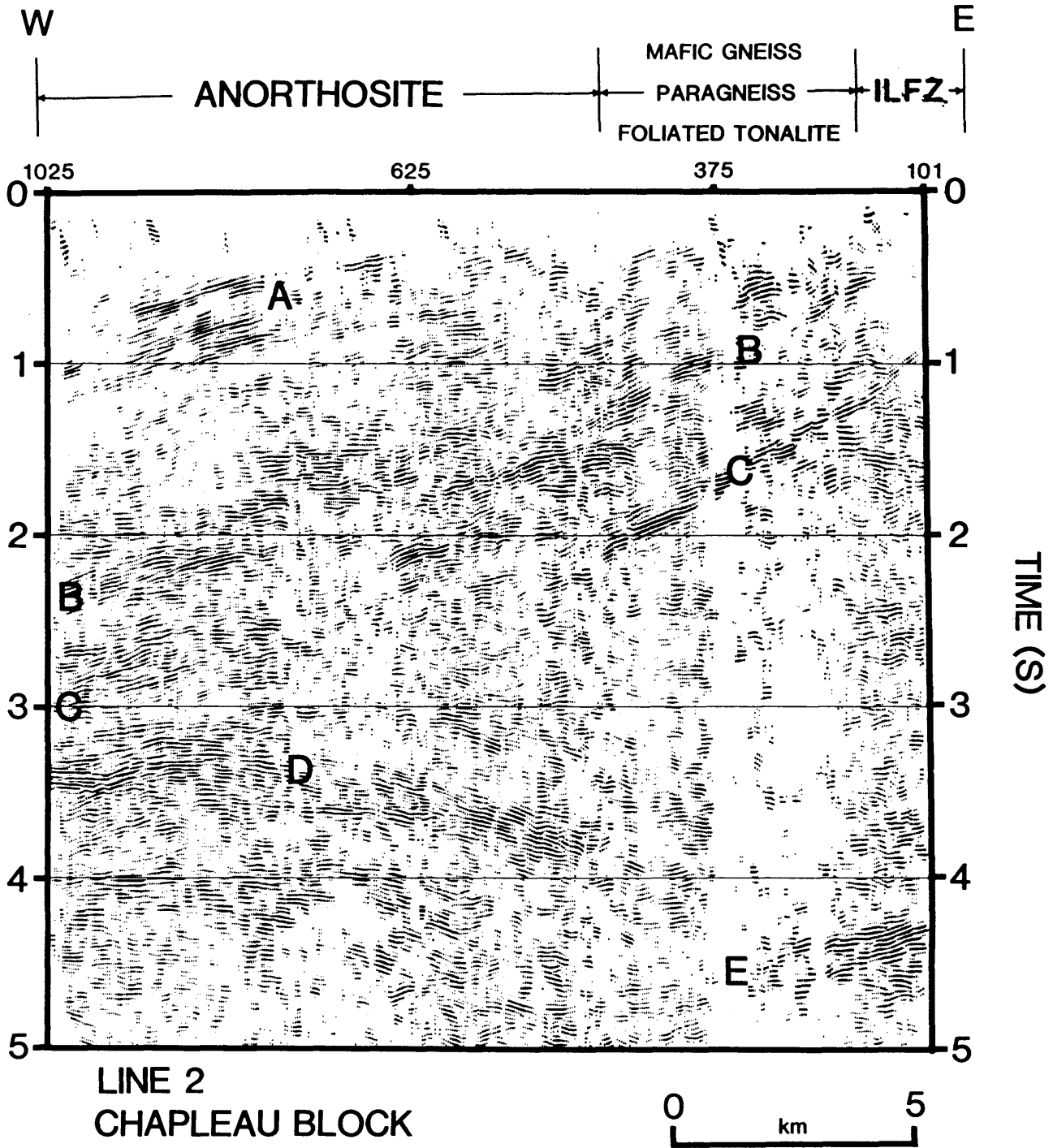
Figure 5.1: Map illustrating the location of line-2 high resolution and local geology (after Percival and Card, 1983) of the Chapleau block. Note location of ILCZ. Adapted from Cook, (1985).

## Data Description and Interpretation

### Line 2 High Resolution

Unmigrated high resolution data are displayed to 5.0 s two-way time (about 15-17 km using an average velocity of 6.0-6.5 km/s) in Figure 5.2. The data quality is excellent, with numerous reflections clearly visible between 0.2 and 4.5 s (0.6 to 13.5 km). Two reflection orientations are dominant. Between 0.2 and about 3.0 s, reflections are predominantly west dipping; below 3.0 s reflections are subhorizontal to east dipping, implying a major transition between the two orientations. In the shallow part of the section a westward thickening wedge of reflections has its base delineated by reflection C. Reflection C arrives at 0.8 s (2.4 km) on the east side of the section and dips to about 3.0 s (9.0 km) on the west. Above reflection C, reflection B dips from 0.4 s (1.2 km) on the east, to 2.3 s (7.0 km) on the west. Closer to the surface a is zone of layered reflections (A on Figure. 5.2). The top of this zone dips westward from 0.2 s (600 m) under V.P. 501, to about 0.8 s (3.6 km) on the west. The base of reflection zone A dips from about 0.6 s beneath V.P. 501 to about 1.2 s on the west end of the profile. The dip of this highly reflective zone is discordant to the

Figure 5.2: (next page) High resolution CMP seismic section (unmigrated and coherency filtered) along line 2 displayed to 5.0 s two-way time. Migrated versions only slightly change the geometrical relationships of the shallow reflectors and are not shown since they degrade the image quality due to the discontinuous nature of many of the reflections. Events A through E are discussed in text. Processed trace spacing is 10 m. Displayed trace spacing is 30 m. Zero time on section represents a datum of 400 m above sea level. Data are plotted 1:1 for an average velocity of 6.0 km/s.



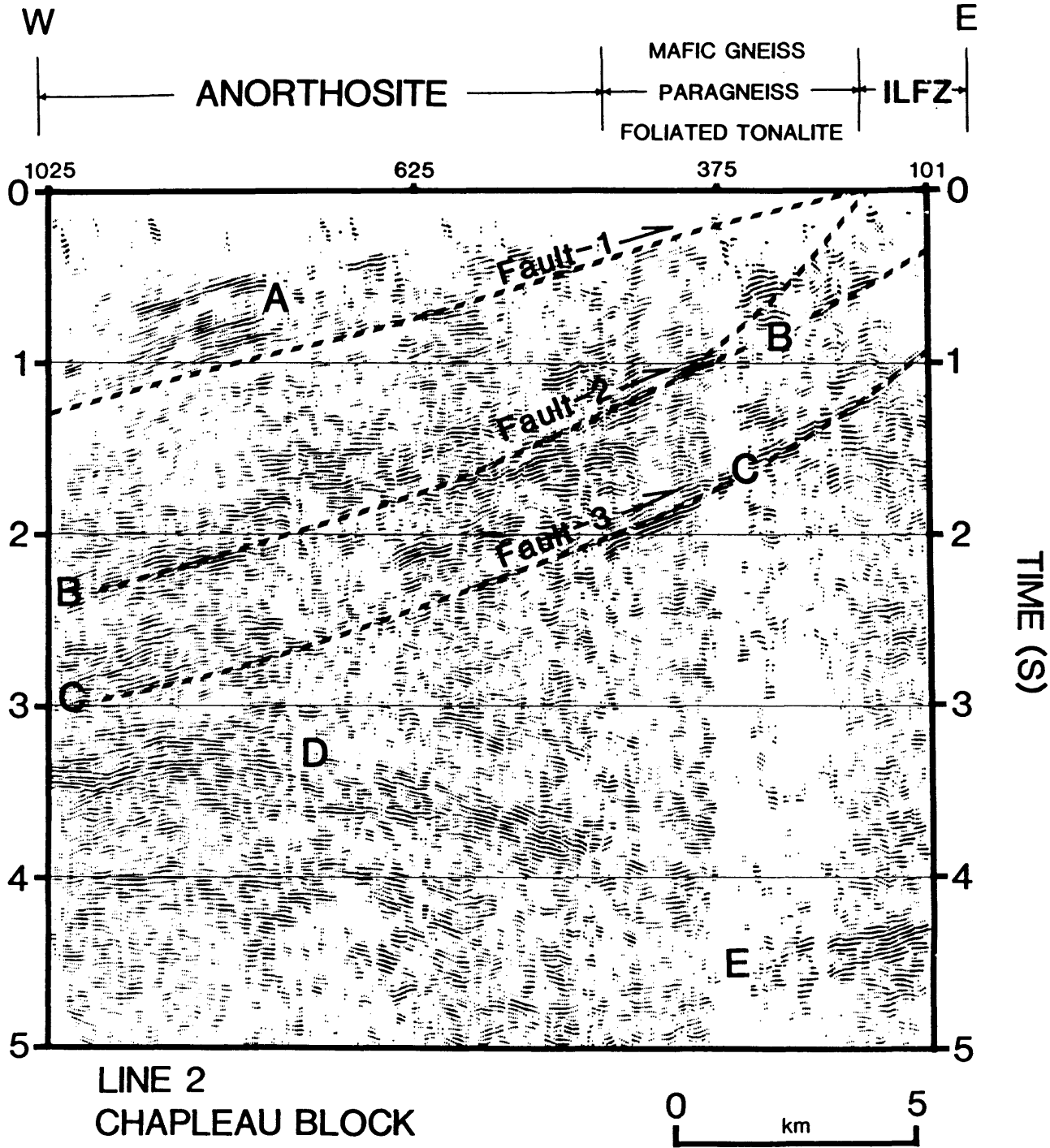


underlying B and C reflections, implying another structural boundary between them.

Beneath the wedge of west dipping reflections, most events have sub-horizontal or east dipping orientations (Figure 5.2). For example, event D is an arcuate east dipping event located between 3.5 and 4.0 s, and event E is a sub-horizontal to slightly west dipping arrival at 4.3 s between V.P. 101-250.

The most significant events supporting the interpretation of southeast-verging thrust faulting are the west dipping events A, B and C. B and C are interpreted as fault plane reflections and A is interpreted as layering that is bounded by a major fault below (Figure 5.3). These boundaries (faults 1, 2 and 3 in Figure 5.3) invariably separate reflections with differing geometry; in some areas they can be projected to within a short distance of surface features. For example, the top of reflection zone A projects to the surface near the contact between Shawmere anorthosite complex and surrounding interlayered mafic gneiss, paragneiss and tonalitic gneiss (V.P. 420); the base of the layering appears to project to the surface near the west side of the ILFZ (V.P. 150; Figure 5.3). Unless the layering turns over and does not actually reach the surface, the highly reflective nature of A likely originates from the lithological contacts between the various gneissic rocks (Green et al, 1989). Based on the

Figure 5.3: (next page) Line 2 high resolution with the interpretations of faults 1, 2 and 3.



correlation between the surface position of ILFZ and truncations of sub-horizontal events beneath A, a detachment that carries the mafic gneiss and tonalite is interpreted to exist at the base of A (fault 1 on Fig. 5.3).

Listric, west dipping reflections B and C project to the surface east of the seismic profile. These events are likely reflections from sheared rocks within and east of the ILFZ. The highly reflective nature of these two events likely result from two effects: the juxtaposition of rocks of differing lithology and metamorphic grade, and velocity anomalies associated with the shearing of the rocks, each of these causing acoustic impedance boundaries (Fountain et al., 1984; Green et al., 1989).

The reflection geometry allows for at least two interpretations of these reflections. In the first, C could be the easternmost detachment (fault 3 on Figure 5.3) of the ILFZ. This fault separates a horse of granodiorite from the granodiorite of the Abitibi belt proper. In this interpretation reflection B would be an additional, but probably minor, fault (fault 2 on Figure 5.3) within ILFZ. Alternatively, reflection B could represent the easternmost fault of the ILFZ. In this case, reflection C would be from a deeper fault, possibly a blind thrust, that projects into the Abitibi belt east of the ILFZ.

The exact relationship between the faults of the ILFZ and the reflections is uncertain in the absence of information

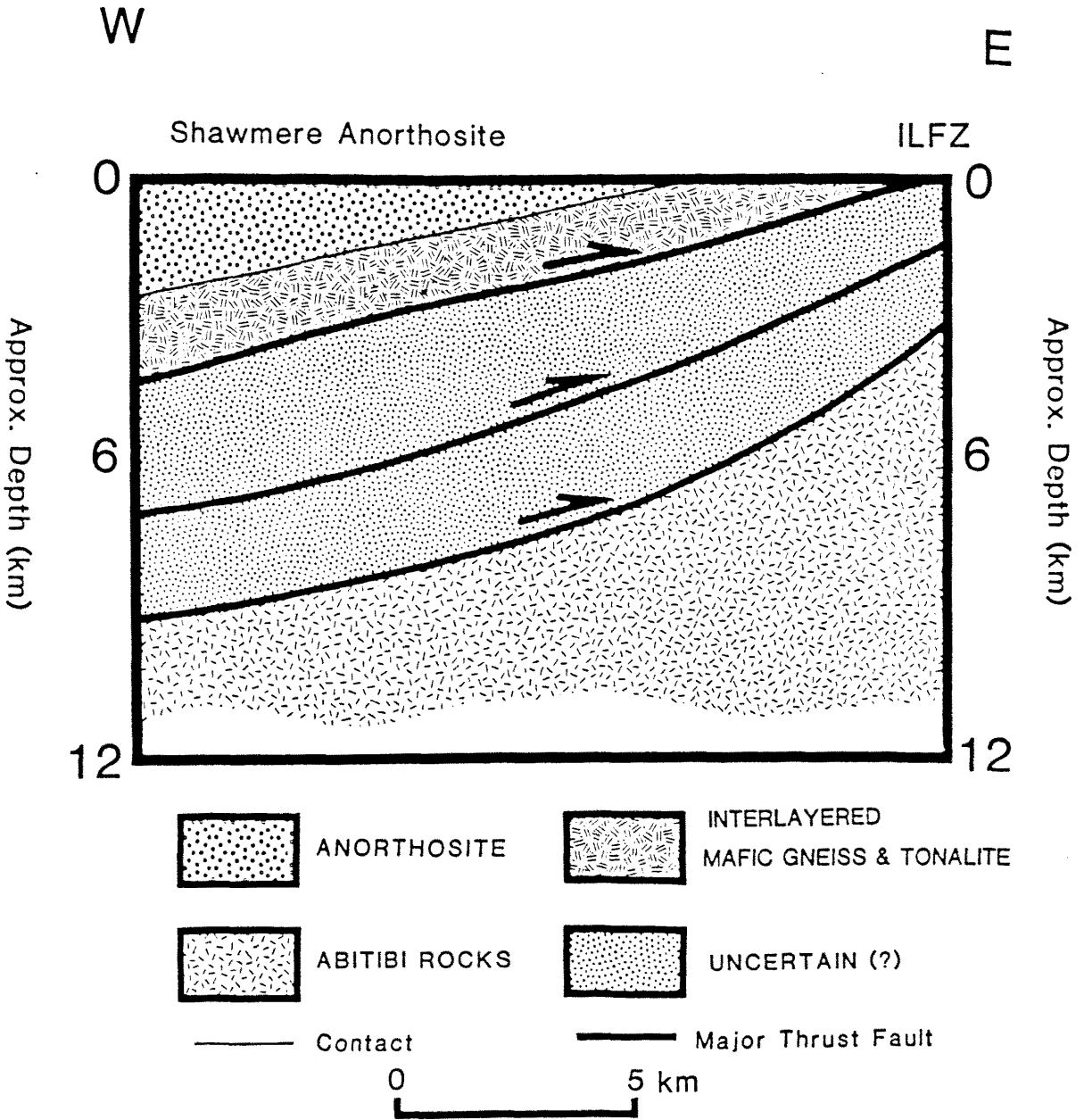


Figure 5.4: Geologic interpretation of line 2 high resolution.

that allows a direct tie of B and C to surface features. The complex reflection geometries suggest an imbricate nature of the faulting and thus implies that additional faults are probable near and within the ILFZ. Figure 5.4 shows a generalized geologic cross section beneath line 2.

Events D and E almost certainly image structures below the KSZ. Event D collapses on migrated versions of section, thus the arcuate nature of D is believed to be largely due to diffracted energy from a source near the west side of the profile at about 3.2 s (10.0 km). Because these features are within the footwall of the KSZ, and, as they do not project to outcrop, they cannot be directly correlated to surface features of the ILFZ or obvious features in the Abitibi Belt. In Chapter 6 some ideas are discussed concerning these events and other Abitibi belt reflections.

#### East-West Regional Data

The relationships of the faults observed on the high resolution profile to the regional structure are clarified on the regional profiles across the Chapleau block. Coherency filtered data from the complete east-west transect show a reflective zone (F1 on Figure 5.5) located at the base of the A reflections on line 2, that dips westward on lines 3 and 4 to at least V.P 1101 on line 4 at 3.8 s (12.0

km). Above F1, west of line 2 the reflections have broad overlapping domal geometries; below F1 the reflections are generally subhorizontal.

The zone of shallow reflections (A on Figure 5.2) associated with the interlayered mafic and tonalitic gneiss changes rather abruptly from west dipping under line 2, to slightly east dipping under line 3 at about 1.0 s (A on Figure 5.5). Below this east dipping zone, reflections are horizontal or dip gently westward (Figure 5.5).

At the west end of line 4, F1 becomes discontinuous with a decrease in amplitude. It may continue as faint, steeper-dipping events (labeled R) observed to about 5.0 s (15 km). This steepening of the reflectors could indicate a ramp structure at the west end of the profile.

As on line 2, the regional profiles show a major boundary (F1) separating regions of fundamentally different internal geometry, each characterized by similar reflection orientations. The major discontinuity is thus interpreted as a significant fault zone. It is very likely that it projects into the ILFZ on the east, has a low dip beneath line 3 and the eastern part of Line 4, and appears to ramp deeper into the crust (R in Figure 5.5) on the west side of line 4.

Reflections B and C (Figure 5.2) are also likely to be faults, and they also flatten over a short distance to the west beneath line 3, into a zone of horizontal layers at

Figure 5.5: (next page) Regional seismic data (unmigrated and coherency filtered) along the complete east-west traverse displayed to 6.0 s two-way time. Processed trace spacing is 25 m. Displayed trace spacing is 50 m. Zero time on section represents a datum of 400 m above sea level. Data are plotted 1:1 for an average velocity of 6.0 km/s.



WEST

EAST

MAFIC GNEISS  
PARAGNEISS  
TONALITIC GNEISS  
IVANHOE  
LAKE  
FAULT  
ZONE

ANORTHOSITIC  
GABBRO  
ANORTHOSITIC  
GABBRO

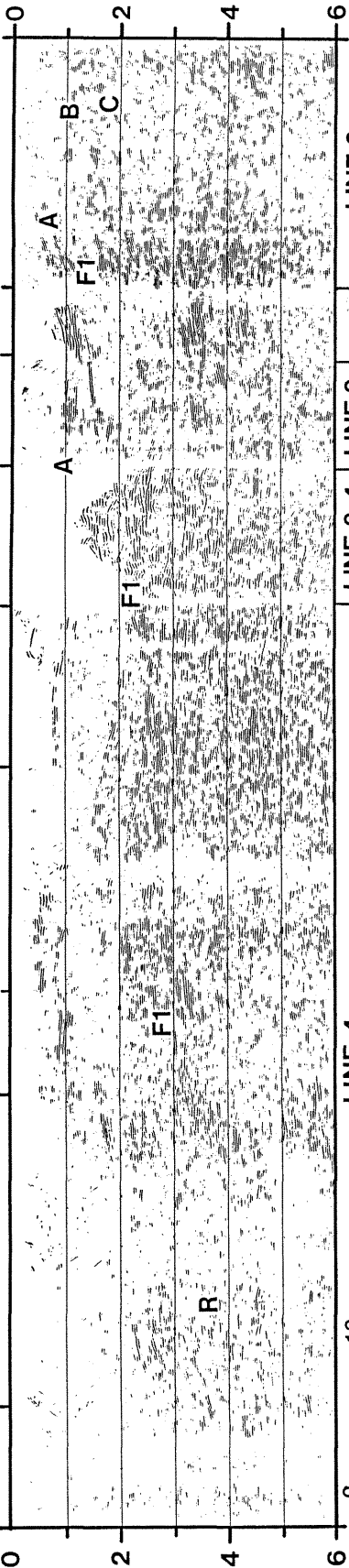
TONALITE  
DIORITE

MAFIC  
GNEISS

DIORITE

PARAGNEISS AND  
TONALITIC GNEISS

1693 1501 1001 501 301 391 181 473 101 0  
Fault



TIME (s)

TIME (s)

0 10  
KM

LINE 4

LINE 3-4

LINE 3

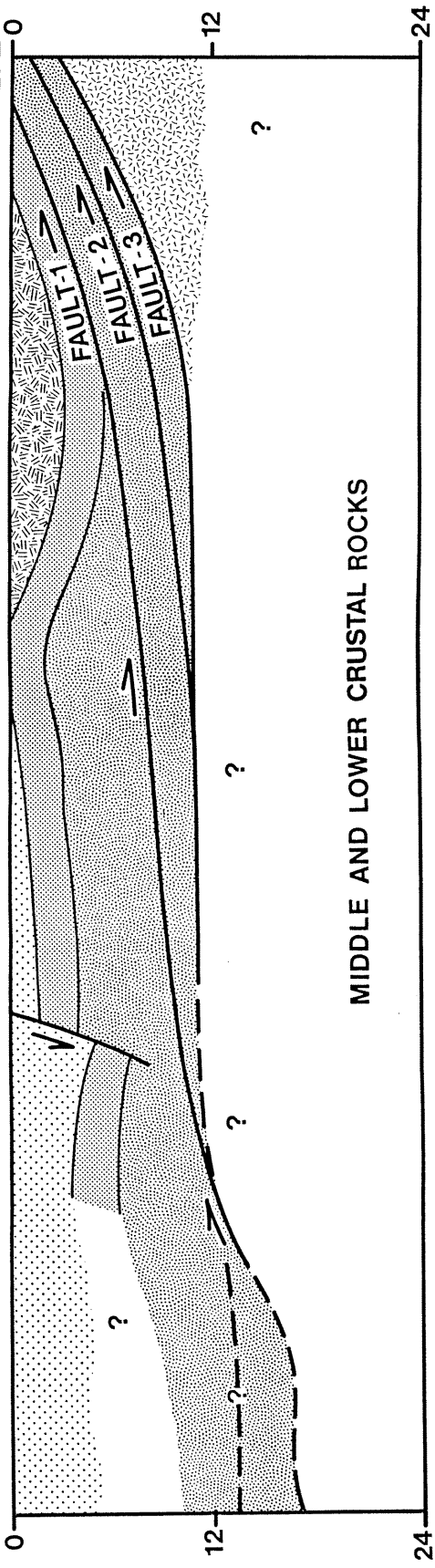
LINE 2

SHOT No.

Figure 5.6: (next page) Interpretation of complete east-west seismic traverse (lines 2, 3 and 4) across the southern KSZ. Three thrust faults with a 'ramp and flat' and a thin upper plate geometry have been interpreted. Normal fault on west end of the cross section is interpreted based on surface location of fault (Figure 1.1) and offset of layered reflections on seismic data (line 4).

1693 1001 301 391 181 473 101 Shot No.

WAWA GNEISS TERRANE SHAWMERE ANORTHOSITE ILFZ



MIDDLE AND LOWER CRUSTAL ROCKS

- 0 10km
- TONALITIC GNEISS PARAGNEISS
- ANORTHOSITE
- INTERLAYERED MAFIC GNEISS PARAGNEISS AND TONALITE
- UNCERTAIN KAPUSKASING ROCKS
- ABITIBI ROCKS
- CONTACT
- MAJOR THRUST FAULT

APPROX. DEPTH (km)

APPROX. DEPTH (km)

about 3.0-3.5 s. Faults 1, 2 and 3 thus may represent imbricates that splay off of a major subhorizontal detachment zone located at about 3.0 - 3.5 s (about 10 km depth) that likely deepens further to the NW. The faults thus have a ramp and flat geometry, similar to many thrust belts in layered sedimentary strata such the Canadian Rocky Mountains (Bally et al., 1966).

### **Discussion and Implications of a Thin Thrust Sheet Model**

A low-angle thrust sheet model differs significantly from previous models (Percival and Card, 1983; Cook, 1985) involving steeper thrusts (See Chapter 2, Fig. 2.1). However, it is not presently known which of the three faults (Figures 5.3 and 5.5) is the principal detachment responsible for transporting the deep crustal Kapuskasing rocks to the surface. One possible model would have fault 1 as an early detachment, followed by faults 2 and 3. Fault 1 would have the maximum offset and faults 2 and 3 would be footwall imbricates (Dahlstrom, 1970) or components of a trailing imbricate fan (Boyer and Elliott, 1982). This interpretation is consistent with the observation that fault 1 clearly underlies the highest-grade Kapuskasing rocks, juxtaposes them with the lower grade Abitibi rocks, and is a

major geometric discontinuity. In this interpretation, folding of some of the domal rocks of the Wawa gneiss terrane could be explained as deformation in the hanging wall of fault 1. Reflections (A on lines 2 and 3) representing the high grade gneisses in the Kapuskasing zone are continuous beneath the Shawmere anorthosite, then reverse orientation and project to the exposed high grade mafic gneiss in the Robson Lake dome, isolating the anorthosite into a bowl like feature (Figure 5.6).

Alternatively, fault 3 could be the major detachment and faults 1 and 2 could be higher level splays. Such an interpretation is consistent with the pronounced change in reflection geometry observed on line 2 high resolution below reflection C (Fig. 5.2), and with the projection of fault 3 to the east side of the ILFZ. In any case the seismic reflection geometry appears to require that the faults flatten westward in to a zone of decollement at about 10-12 (about 3.5 s) km beneath lines 3 and 4.

In order to explain the differential uplift of the KSZ over the Abitibi belt, the major fault must have a trajectory which extends to an appropriate depth to account for the high grade rocks at the surface. Thus, the amount of horizontal transport may be estimated using geobarometric data on the vertical offset and the trajectory of fault 1. Percival and Card (1983) suggest about a 500 MPa (15-17 km) difference between the Kapuskasing zone rocks and the

greenstones in the Michipicoten belt which are at a similar metamorphic grade as the rocks in the Abitibi belt. If the interpretation of a ramp structure at the west end of line 4 is valid, fault 1 reaches the 15-17 km depth (about 5.0 s) beneath V.P. 1500, a distance of about 70 km from the ILFZ along this line of section.

As the orientation of the seismic profile is not perpendicular to the strike of the ILFZ, the minimum amount of shortening was likely less than 70 km. Projecting to a direction perpendicular to strike yields an offset distance of the order of 55 km. However, if there is no ramp at the west end of line 4 and if F1 dips uniformly to a depth of 15-17 km, the minimum amount of shortening would be greater, perhaps as much as 70 km (Percival et al, 1989).

The implications of this magnitude of shortening for the evolution of the KSZ and adjacent areas of the Superior province and the uplift of the high grade metamorphic rocks are profound. The calculated shortening suggests that the detachment extends northwestward beneath the Wawa terrane and Michipicoten belt. Whether such a detachment remains at about 15-17 km (as seen on the west side of line 4; Figure 5.5), or whether it projects to greater depths further northwest is unknown. In any case, however, it appears that much the upper and middle crust of the Superior province was detached from the lower crust during the formation of the KSZ.

The geometry of the faults is similar to that seen in Phanerozoic sedimentary thrust and fold belts, such as the Rocky Mountains, with ramps, flats and imbricate thrusts. The deformation of the KSZ, however, took place within Archean amphibolite and granulite facies rocks. It seems likely, therefore, that deformation of such rocks occurs as it does in low grade, layered rock with the rheological properties of the layering likely determined by lithologic variations, the presence of fluids, and temperature.

### **Summary of Chapter 5**

Lithoprobe seismic reflection profiles have revealed the geometry of the faults that are responsible for the emplacement of the lower crustal rocks of the Kapuskasing structure. Three significant southeast verging, low angle thrust faults that likely merge into a horizontal detachment have been observed. Their geometry resembles a 'ramp and flat' style of deformation, resulting in a thin upper plate above the upper most detachment. The minimum horizontal shortening along a NW-SE direction is estimated at about 55-70 km. The implications of this geometry are that a large portion of the upper-middle crust beneath the Superior province was detached from the underlying lower crust during

formation of the KSZ, and that high grade rocks may deform into structures that strongly resemble those of layered rock such as in younger supra-crustal thrust and fold belts.



## **CHAPTER 6: THREE DIMENSIONAL STRUCTURE OF THE CHAPLEAU BLOCK**

### **Introduction**

In this chapter the interpretation of low angle thrust faults beneath the KSZ will be expanded to incorporate the remaining regional profiles (lines 1, 5 and 6) from the Chapleau block. With the addition of these lines, time structure maps of the major fault surface have been constructed, allowing the three dimensional subsurface structure of the Chapleau thrust block to be determined. Finally, some comments are made concerning some of the seismic geometries observed in the adjacent Abitibi belt and how these might be related to the KSZ.

### **Data Description**

The faults beneath the KSZ are not as well imaged near the surface on lines 1, 5 and 6 as they are on the east-west transect; however, as the reprocessing of line 2 regional improved the shallow image along that line, it is likely that similar reprocessing efforts on these regional lines will also improve the correlation of the reflections

with the surface features. Nevertheless, the initial stack sections still provide some constraints on the 3-D structure. The interpretation of the faults are constrained by the surface location of the ILFZ, various line ties, and the reflection geometry. Line 1 begins in the Abitibi belt in the south, where exposures include homogeneous granite (Percival and Card, 1983; 1985), and terminates about 100 km to the north within the KSZ (Figure 1.1). It crosses the ILFZ at about V.P. 1550, then extends north to intersect with line 4 at about V.P. 601 near the Robson Lake structure. Line 5 begins in the west, within the Shawmere anorthosite complex, crosses the ILFZ about 5 km to the east and then terminates 25 km to the southeast in the Abitibi belt. Line 6 begins in the south within the Abitibi belt and heads northwest for 50 km into amphibolite grade tonalite, obliquely crossing the ILFZ at V.P. 550.

All of these lines show that the greatest amount of reflectivity and the largest structures are within the Abitibi belt south or east of the ILFZ. On lines 1 and 6 zones of north and northwest dipping reflections (Figures 6.1 and 6.2) project to the surface beneath outcrops of felsic gneiss and homogeneous granite. There is currently no surface evidence for any faults or exposures of high grade rocks related to the Kapuskasing structure south of ILFZ on lines 1 and 6, thus any reflections south of the ILFZ are believed to be imaging structures within the

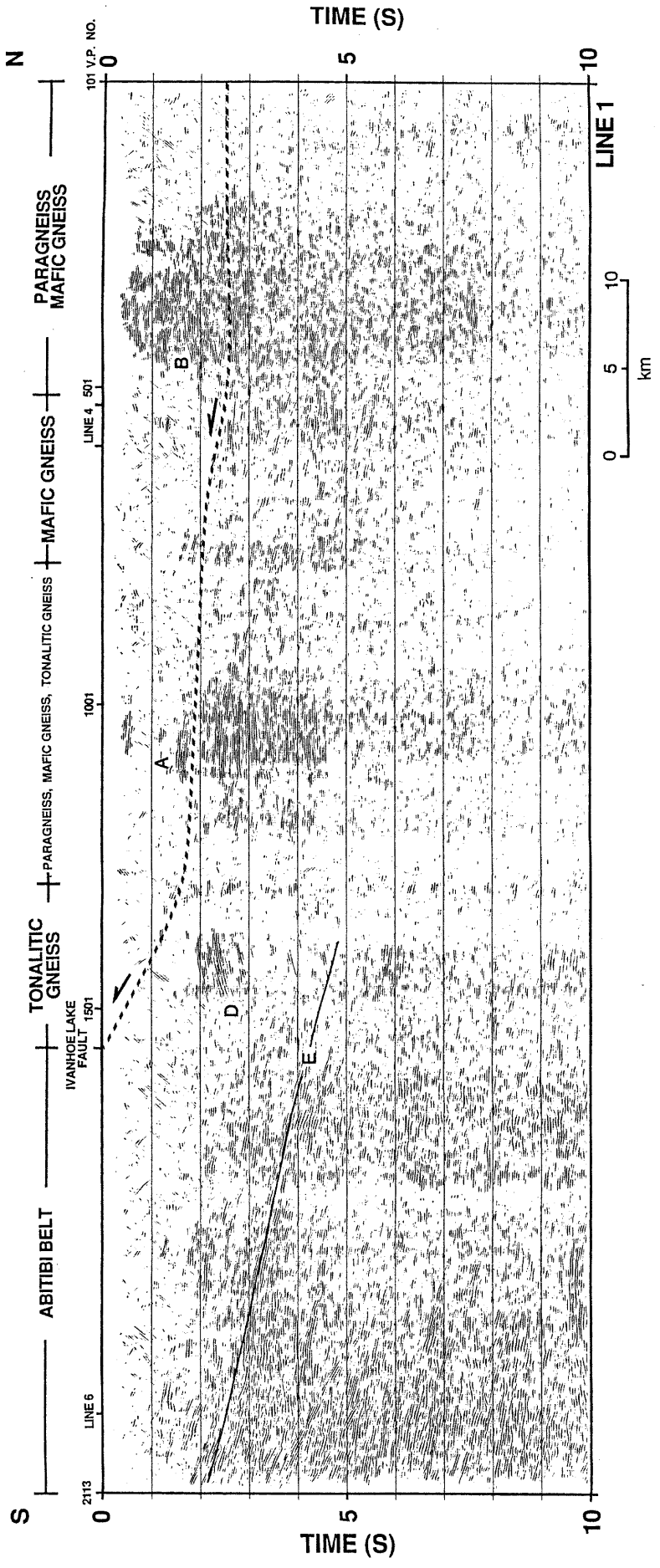
Abitibi belt that are not directly related to the Kapuskasing structure.

### Line 1 Regional

Beneath the KSZ (north of the ILFZ) the reflection geometry on line 1 is discontinuous and for the most part subhorizontal to slightly northward dipping down to about 5.0 s (Figure 6.1). Two prominent zones of reflectivity can be observed. Between V.P.'s 900 and 1100 subhorizontal reflections (A) underlie a dome of tonalitic gneiss. In the north another highly reflective zone of subhorizontal events (B) is seen between 0.3 and 3.0 s. Slightly north of the surface expression of the ILFZ, at about 2.2 s, an arcuate south dipping reflection (D) is located in a similar structural position as the arcuate reflection (D) seen on line 2 (Figure 5.2), suggesting a common geometrical relationship.

No reflections can be correlated exactly with the fault zone; however, its position is constrained using the tie with the F1 surface on line 4, the ILFZ on the surface along line 1 and the subhorizontal reflections (A) on line 1. Fault 1, interpreted on line 4, ties with subhorizontal energy on line 1 at about 2.5 s. It is not certain how many faults exist beneath line 1, but the position of the lowest

Figure 6.1: (next page) Regional seismic data (unmigrated and coherency filtered) along the Line 1 displayed to 10.0 s two-way time. Processed trace spacing is 25 m. Displayed trace spacing is 50 m. Zero time on section represents a datum of 400 m above sea level. Data are plotted 1:1 for an average velocity of 6.0 km/s.



level of detachment can be inferred and is interpreted as the dotted line on Figure 6.1. As on the east-west transect (lines 2, 3 and 4) the fault is apparently low angle, resulting in a thin plate above the detachment.

### Line 6 Regional

Line 6 (Figure 6.2) displays similar reflection geometries to those on line 1. The subsurface of the Abitibi belt is again highly reflective with prominent northwest dipping reflections; however, the apparent dips on these reflections are not as steep as those on the south end of line 1.

Northwest of the ILFZ, below about 2.0 s (6 km), the geometry is dominantly subhorizontal with a few southeastward dipping reflections. Above 2.0 s, reflections dip slightly northwestward and project to the surface near the Ivanhoe Lake fault (A in Figure 6.2). These northwest dipping reflections constrain the position of the fault, which again flattens over a short distance to the northwest.

Figure 6.2: (next page) Regional seismic data (unmigrated and coherency filtered) along the line 6 displayed to 10.0 s two-way time. Processed trace spacing is 25 m. Displayed trace spacing is 50 m. Zero time on section represents a datum of 400 m above sea level. Data are plotted 1:1 for an average velocity of 6.0 km/s.

SE

ABITIBI BELT

TONALITIC GNEISS

NW

IVANHOE LAKE  
FAULT

LINE 1

601

1101 V.P. NO.

0

0

A

B

TIME (S)

TIME (S)

5

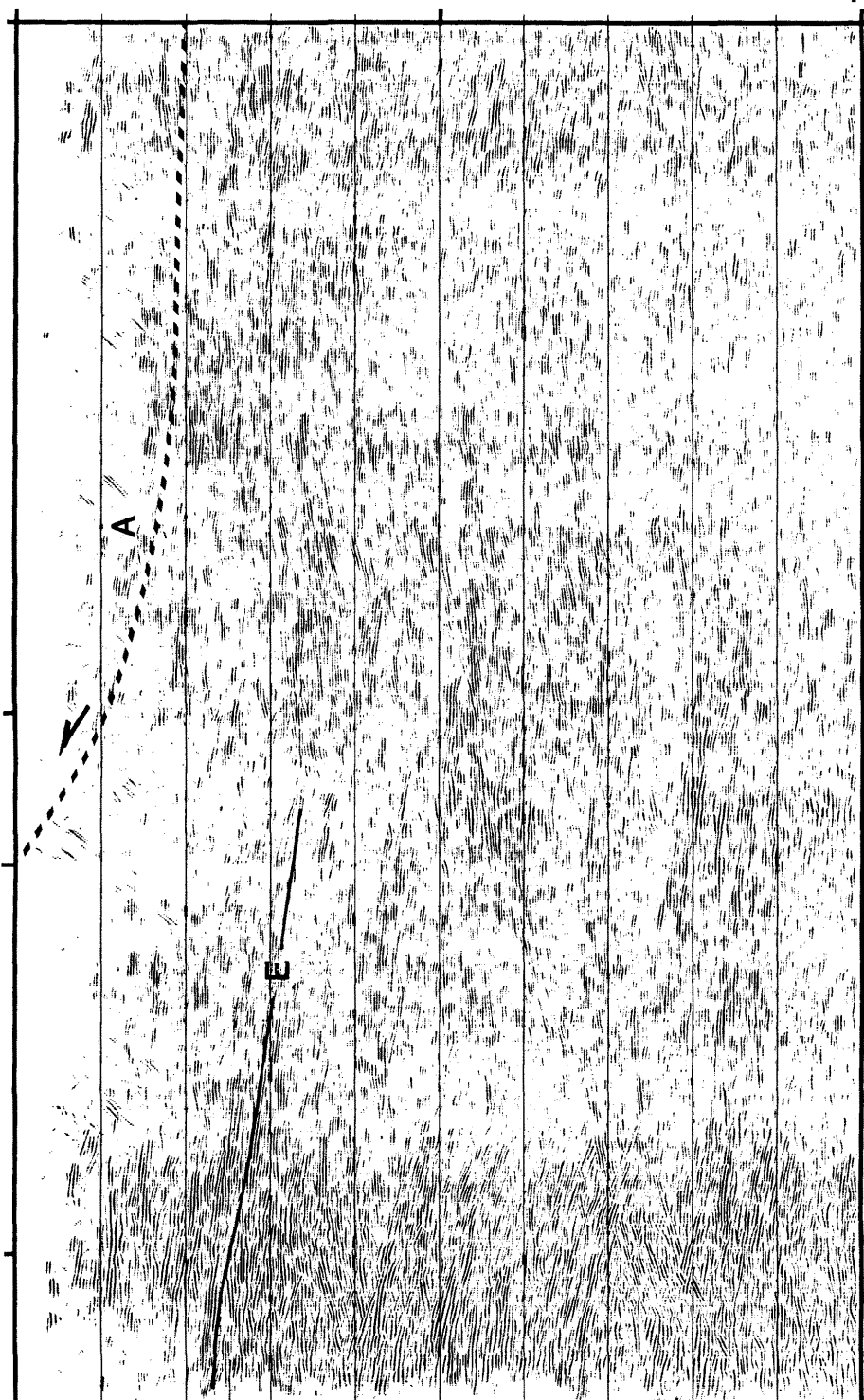
5

10

10

LINE 6

0 5 10  
km





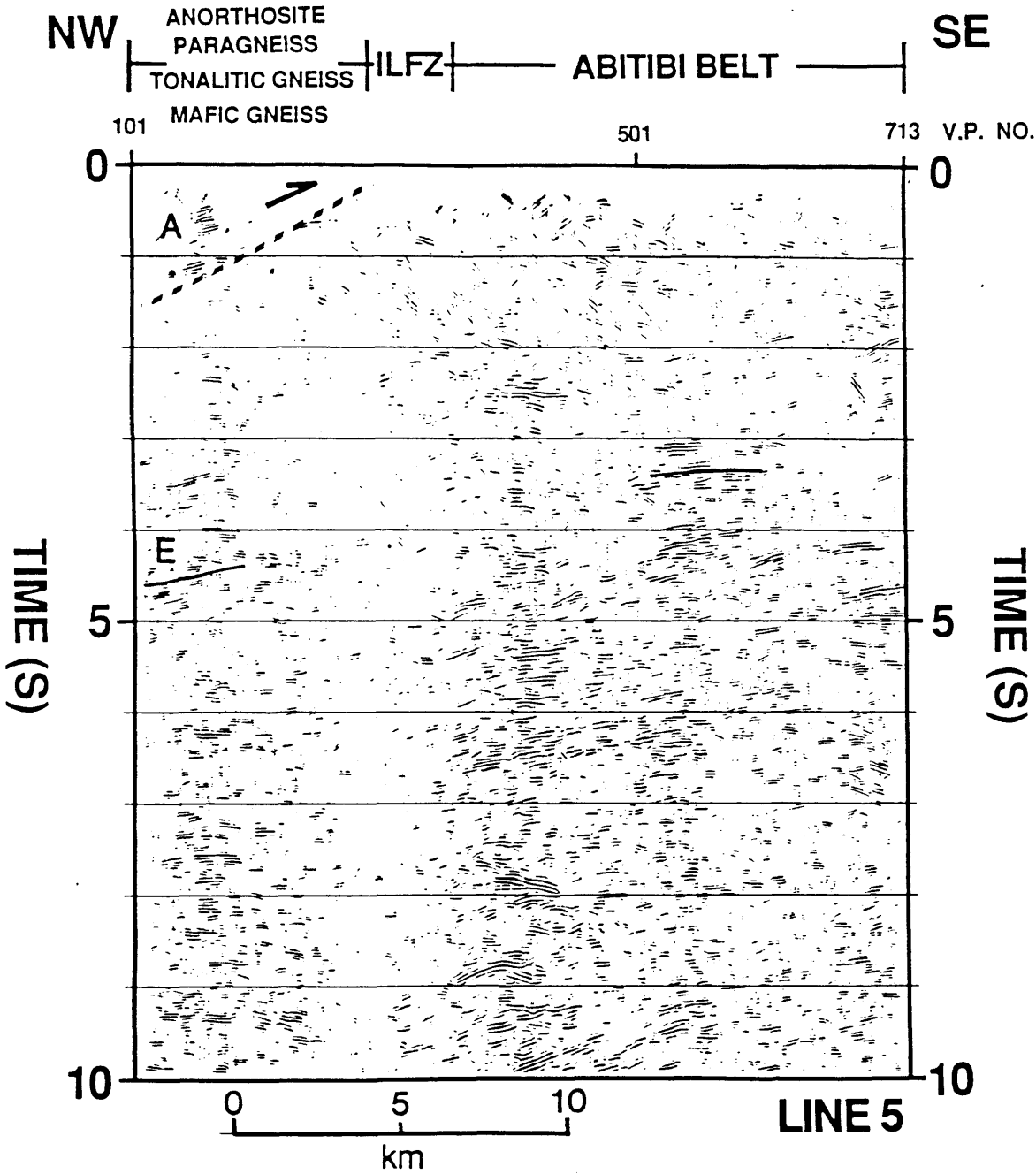
### Line 5 Regional

As with lines 1 and 6, line 5 shows that the Abitibi belt rocks beneath and adjacent to the KSZ are very reflective. In the northwest, beneath the anorthosite, westward dipping events (A on Figure 6.3) project to the surface in the vicinity of the ILFZ. These events are similar to the A layered reflections on line 2 representing the various gneissic rocks and are thus interpreted to be underlain by fault 1 (Figure 6.3). No convincing evidence is seen for any additional faults related to the ILFZ on this profile.

### **3-D Geometry of Chapleau Thrust Block**

Although images of the fault(s) bounding the Chapleau block are not as clear on regional lines 1, 5, and 6 as they are on the high resolution profile, the reflection configuration provides some constraints on the position of the fault and related geometries and allows the 3-D subsurface geometry to be outlined. Time structure maps of the fault 1 surface on the east-west transect and the detachments interpreted on lines 1, 5, and 6 have been constructed (Figures 6.4 and 6.5) using the Landmark Graphics workstation at The University of Calgary. The maps

Figure 6.3: (next page) Regional seismic data (unmigrated and coherency filtered) along the line 5 displayed to 10.0 s two-way time. Processed trace spacing is 25 m. Displayed trace spacing is 50 m. Zero time on section represents a datum of 400 m above sea level. Data are plotted 1:1 for an average velocity of 6.0 km/s.



show that the isochron contours of the Kapuskasing thrust block are generally parallel to the surface expression of the ILFZ. The ramp inferred on line 4 is nicely displayed in perspective view looking from the northeast direction (Figure 6.5). This ramp likely follows a NNE trend (Figure 6.4).

The contour maps show the subsurface orientation of the Chapleau block thrust surface and imply that the direction of faulting was to the southeast. Estimates of the minimum amount of shortening require projection to the true dip direction. As suggested in Chapter 5, and supported by the 3-D results, projection from the east-west (lines 2, 3 and 4) to N45°W (Figure 6.4) is appropriate.

### **Some Comments on the Abitibi Belt Reflections**

The highly reflective and complex nature of the seismic images from the Abitibi belt beneath the ILFZ are in many ways more impressive than the near surface Kapuskasing structures. Although no ties with surface features are possible at present, some speculative statements can be made about the significance of the deeper structures. The fact that similar reflection geometries are observed beneath the ILFZ on lines 1, 2 and 6 implies that the Abitibi belt

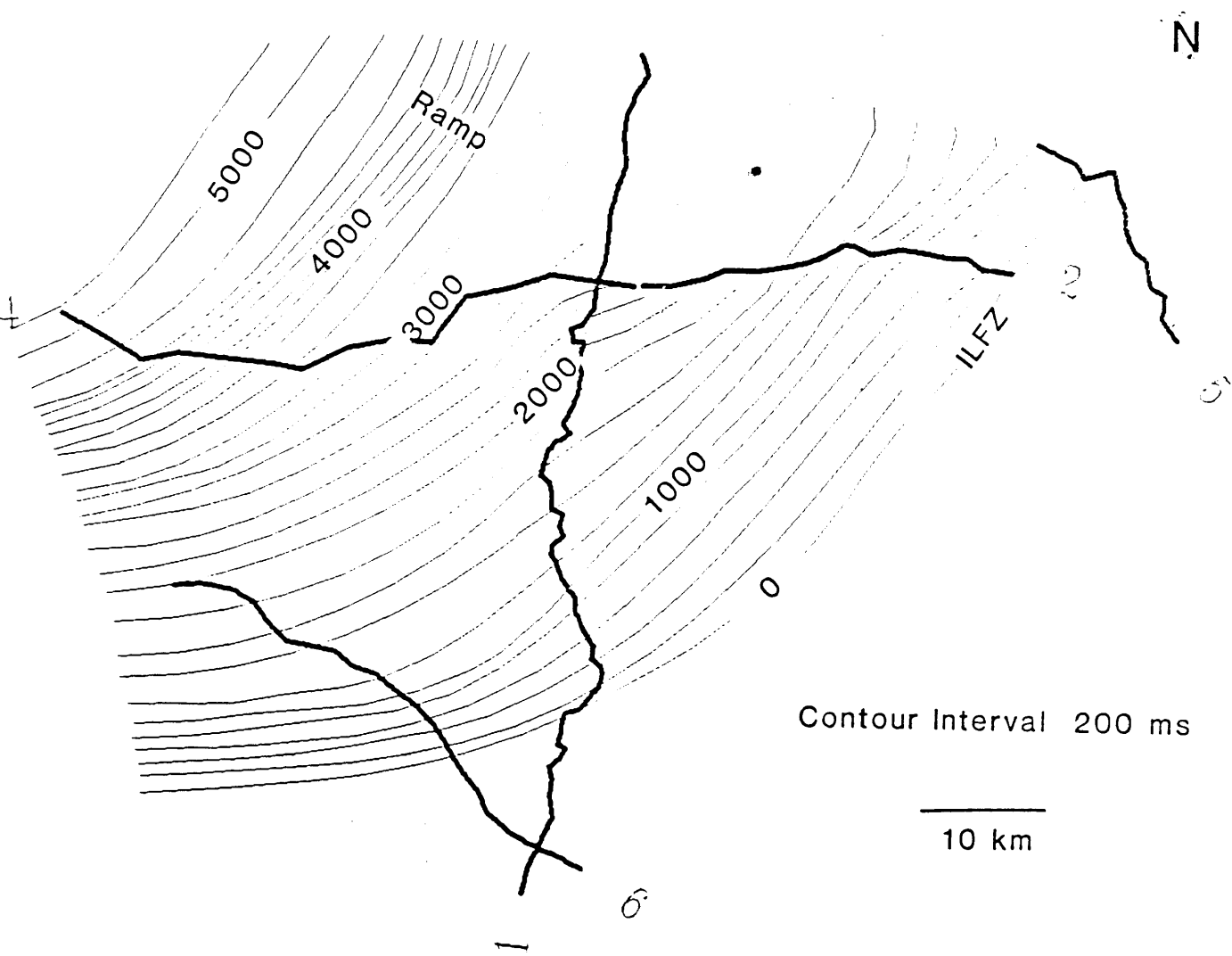
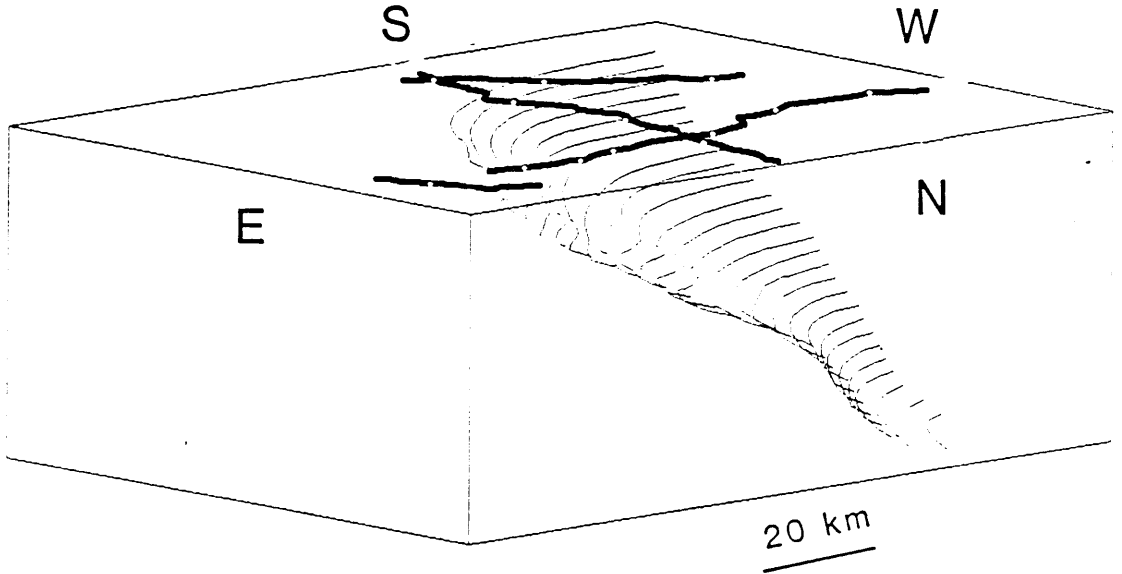


Figure 6.4: Time structure map of Chapleau thrust block



Contour Interval 200 ms

Vertical Exaggeration Approx. 2.5 times

Figure 6.5: Perspective map of Chapleau thrust block as viewed from the northeast.

reflections are present over a wide area; reflections E on lines 1 and 6 (Figure 6.1 and 6.2) occur in the same position with respect to the ILFZ as reflections E on line 2. Line 5 also contains events that may be related to these and are labeled E on Figure 6.3.

Figure 6.6 shows a time structure map of these events. The actual time picks of these events are shown on the corresponding seismic sections (Figures 5.3, 6.1, 6.2 and 6.3). Comparison of this map (Figure 6.6) with the contour map of the Kapuskasing thrust block (Figure 6.4) shows that on a regional scale the shallow ILFZ surface and the deep Abitibi reflections are generally parallel. Two possible interpretations are: 1) the Abitibi structures were pre-existing and were not formed along with the KSZ or, 2) these structures were formed at the same time as the KSZ. If they were a pre-existing structure, such as a large scale crustal ramp, they may have controlled the emplacement and the orientation of the KSZ. Alternatively, if they formed at the same time as the Kapuskasing uplift, they may have been related to even deeper level detachments associated with the KSZ that project past the ILFZ, suggesting the actual front of the deformation involved in the formation of the KSZ extends further east and south into the Abitibi belt. As mentioned previously, there is currently no evidence for faults or large scale folds east or south the ILFZ associated with the KSZ; however reevaluation and more 6.5

N

E

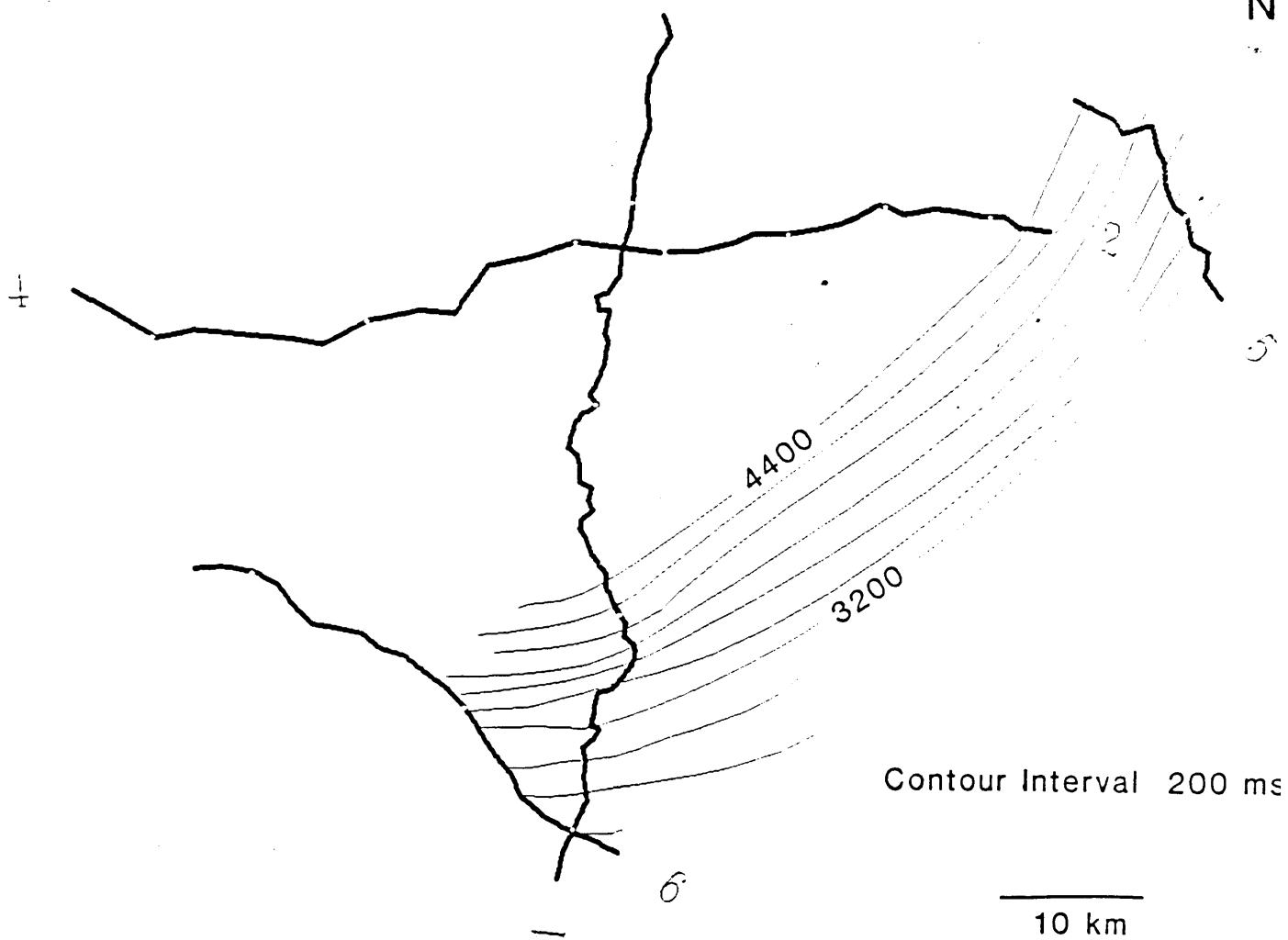


Figure 6.6: Time structure map of Abitibi belt reflection E.



mapping of the surface geology in these regions may give some insight to these large structures.

### **Summary of Chapter 6**

On lines 1, 5 and 6, the reflection geometry beneath the KSZ is very shallowly dipping, supporting the interpretation of low angle thrust faulting. By using the reflection geometry, line ties, and the surface location of the ILFZ, the fault surface beneath the Chapleau thrust block has been mapped. The maps show that on a regional scale the time structure contours parallel the ILFZ and that the transport of the thrust block was to the southeast.

The most pronounced structures imaged by the Kapuskasing seismic data come from the adjacent Abitibi belt. Although no ties with outcrop can presently be made, contour mapping of these reflections shows that the structures generally parallel the ILFZ surface. Hence, these structures may have been pre-existing and thus influenced the emplacement of the KSZ, or they may have been associated with deeper level detachments that occurred during the Kapuskasing uplift and project past the ILFZ into the Abitibi belt.

## CHAPTER 7 RECONSTRUCTIONS

### Introduction

Chapters 5 and 6 have described the seismic reflection geometry and discussed the thin (about 10 km) thrust sheet emplacement of the middle to lower crustal rocks of the KSZ. Based on the surface geology and the seismic geometry, a cross section has been proposed that includes at least three faults with a minimum amount of shortening estimated at 55 km (Figure 5.6). This chapter further discusses the implications of the geometries seen on the seismic data and makes some preliminary attempts at steps towards a schematic reconstruction of the cross section. Only the east-west seismic profile, projected onto the true dip direction, will be used for the reconstructions, as it best represents the fault geometry; however, the 3-D geometry provided by the other data permit projections to true dip. Using the available constraints and some assumptions, three scenarios are presented. In the first two models, fault 1 is assumed to be the principal detachment with the most displacement. In the third model both fault 1 and fault 3 have a significant amount of displacement.

## Reconstruction Constraints and Assumptions

The geophysical and geological data provide strong constraints on the proposed cross section (Figure 5.6). These are summarized below from previous chapters.

The seismic reflection data provide the following geometric constraints:

- 1). The inferred trajectories of fault 1 and fault 3.
- 2). The formation of a hanging wall syncline beneath the anorthosite complex.
- 3). The major detachment (fault 1) paralleling the interlayered high grade gneisses beneath line 2 (Figure 5.4), then cutting below them on line 3, which necessitates the presence of at least one ramp some where to northwest.
- 4). The steepening of reflections observed on the west end of line 4, suggesting the possible presence of a ramp about 70 km along the direction of the seismic profile or about 55 km to the NW in the true dip direction.

The geobarometric data on the amount of vertical uplift between the Abitibi belt and the KSZ are not well constrained. Scattered measurements from the highest grade rocks in the Kapuskasing zone proper range from 700-900-MPa (7-9 kbar) indicating burial depths of 24-30 km. Measurements from Michipicoten belt greenstones near Lake Superior suggest 200-300 MPa (2-3 kbar) indicating burial

depths of 7-10 km (Percival and Card, 1983; Percival and Green, 1988). No geobarometric measurements are available from the Abitibi belt east of the KSZ. Based on these measurements the present amount of vertical uplift between the Kapuskasing gneisses exposed at the surface and the lower grade Wawa gneisses range between minimum and maximum values of 14 and 23 km. For the reconstructions discussed here a moderate value of 15-17 km of vertical uplift will be used.

Along with the these constraints, the following assumptions will be used:

1). Although the east-west transect is not a true dip profile, projection to the true dip direction results in the same geometrical relationships, only over a shorter distance. As there is about a  $35^{\circ}$  difference between the bearing of the east-west seismic profile and the true dip direction of the ILFZ (Figure 6.4), the cross sections have been projected to the true dip direction and structures have been scaled accordingly.

2). The layered reflections observed from the high grade Kapuskasing gneisses on lines 2, 3 and 4 are laterally continuous and can be considered as pseudo-stratigraphy that can be retrodeformed.

3). The middle to lower crustal rocks behave and deform as layered media and the rules of constant bed length and thickness typically used in cross section reconstruction apply (Dahlstrom, 1969). Although this is not strictly valid, any deviation from this assumption would increase the amount of shortening accordingly; the approach taken here is to determine a minimum value of horizontal shortening.

## Conceptual Models

### Models 1 and 2: Fault 1 as the Principal Detachment

One way to explain the interpretation of the hanging wall syncline on the eastern end of the cross section includes deformation over two ramps with the principal detachment having a stair case trajectory (Figure 7.1). In this model fault 1 is the principal detachment and faults 2 and 3 are minor faults that splay off a major detachment at 10 km. The first ramp is the one proposed on the west end of line 4. The interlayered gneissic rocks would have a normal structural level at the base of this ramp, as here they reach the necessary depth of 15-17 km. As fault 1 apparently parallels the high grade gneissic layers and then cuts below them, a second ramp can be predicted further to the northwest. Seismic refraction data (Boland and Ellis, 1989; Figure 7.2) show a large step in the 6.6 km/s mid-crustal velocity contour about 80-90 km northwest of the ILFZ along the true dip direction; such a step may correspond to this second ramp. The hanging wall counterpart to the first ramp has been eroded away and points A - B reconstruct to points A' - B' (Figure 7.1). Formation of the hanging wall syncline would be in response to uplift over the second ramp. The minimum amount of

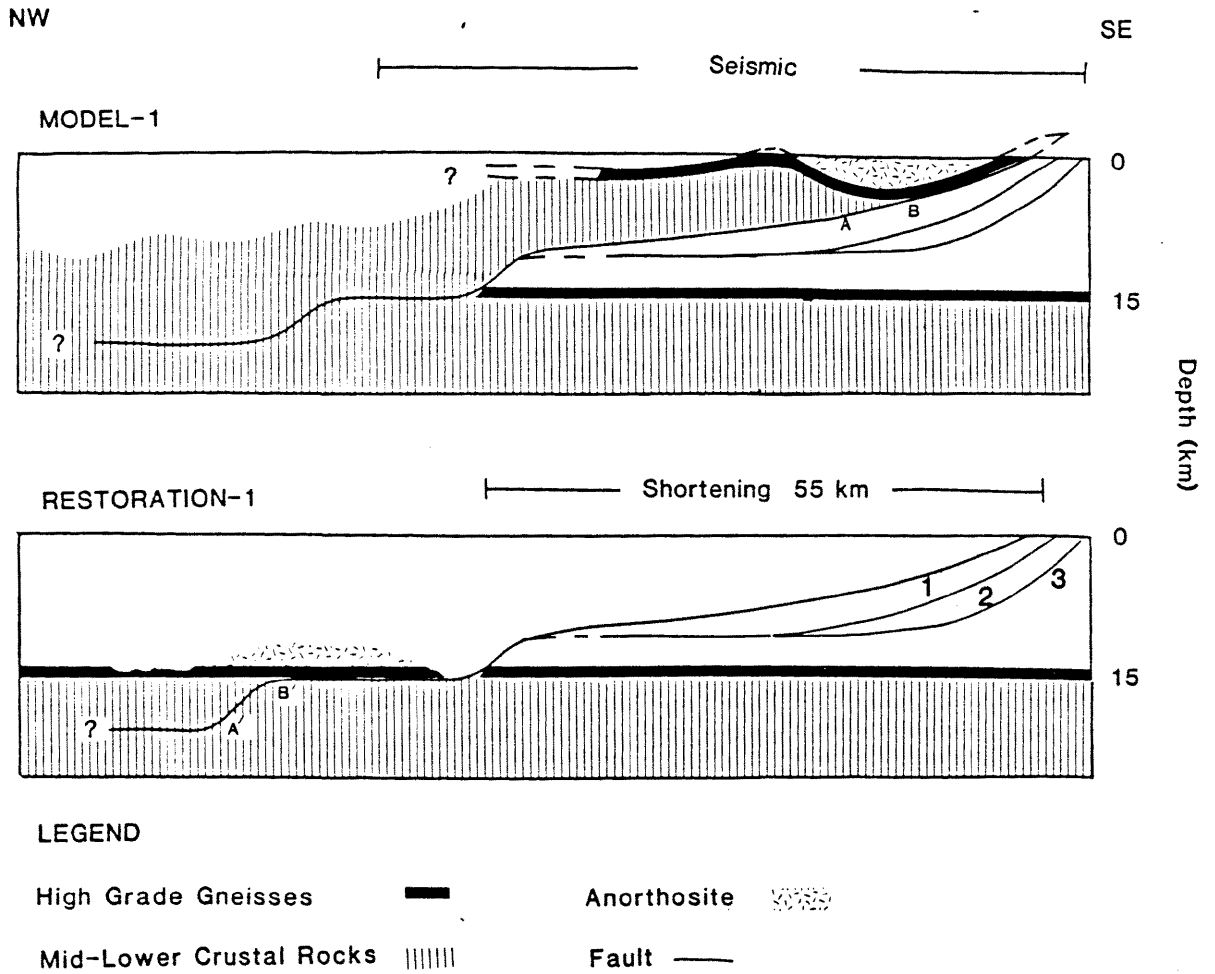


Figure 7.1: Model 1: Fault 1 as the principal detachment with 55 km of shortening.

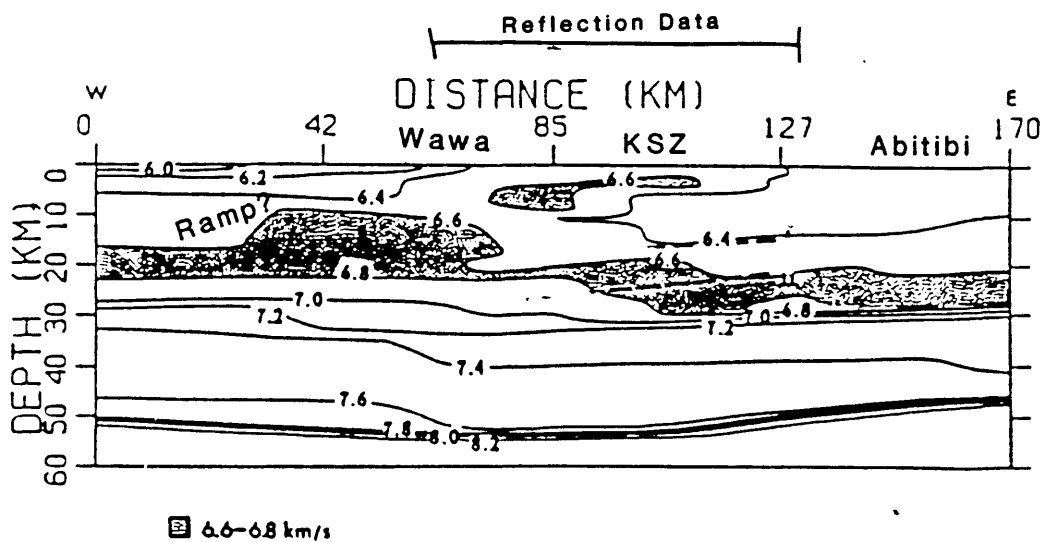


Figure 7.2: Velocity profile across Chapleau block from seismic refraction data (modified from Boland and Ellis, 1989). Step in 6.6 to 6.8 km/s contour may be due to a ramp beneath the western Wawa belt.

shortening with this configuration would be about 55 km as suggested in Chapter 5 (Figure 7.1).

Model 2 is a slight modification of model 1 with no ramp beneath the western end of line 4. In this case fault 1 would reach the 15-17 km level at about 70 km from the ILFZ based on a  $16^{\circ}$  degree average dip (Percival et al, 1989). Nevertheless, as fault 1 apparently cuts below the various gneissic rocks, at least one ramp (A'-B') further westward can be predicted (Figure 7.3). For both models 1 and 2, faults 2 and 3 would be minor faults with little displacement.

### Model 3:

A third model in which both fault 1 and fault 3 have undergone significant displacement is shown in Figure 7.4. In this model fault 3 brings up the high grade gneissic layer a few kilometers, then fault 1 carries it the remaining distance (Figure 7.4). Fault 2 would again have minor displacement. No certain amount of shortening can be determined in this model, but one possible scenario could have about 15 km of displacement on fault 3 and about 70 km on fault 1, with a total amount of shortening of about 85 km (Figure 7.4).



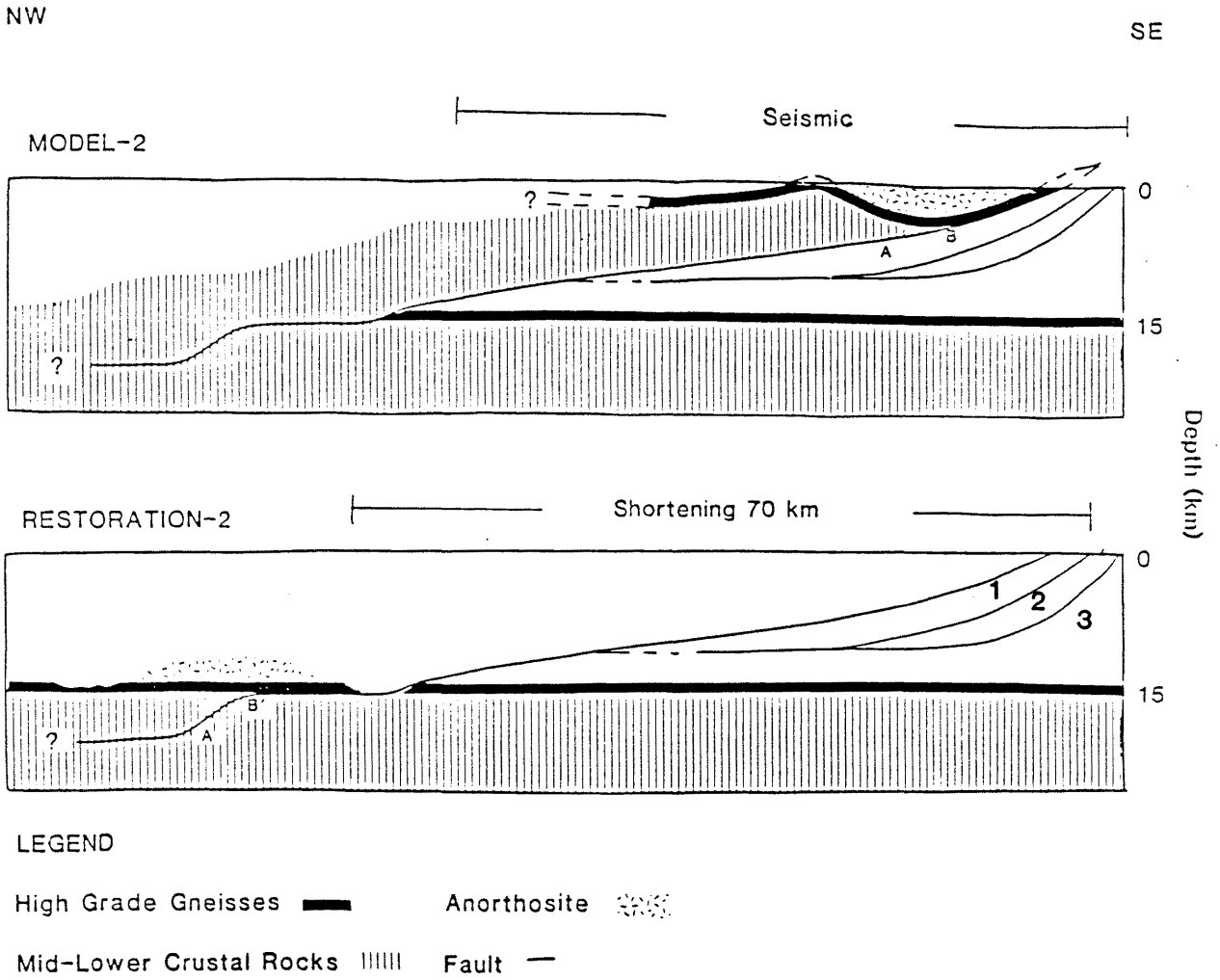


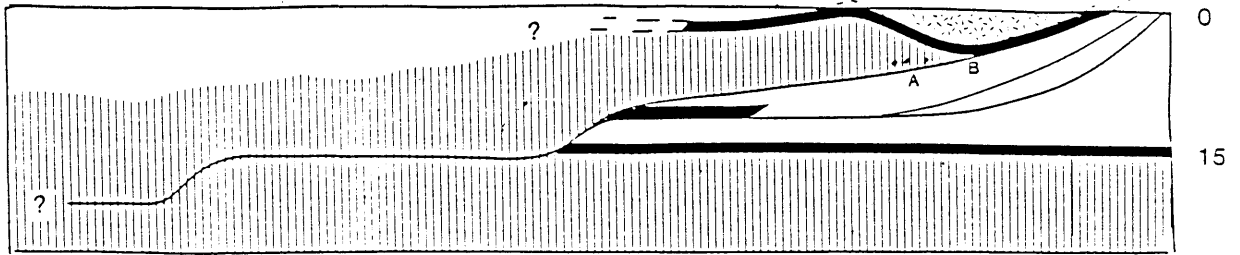
Figure 7.3: Model 2: Fault 1 as the principal detachment with 70 km of shortening.

NW

SE

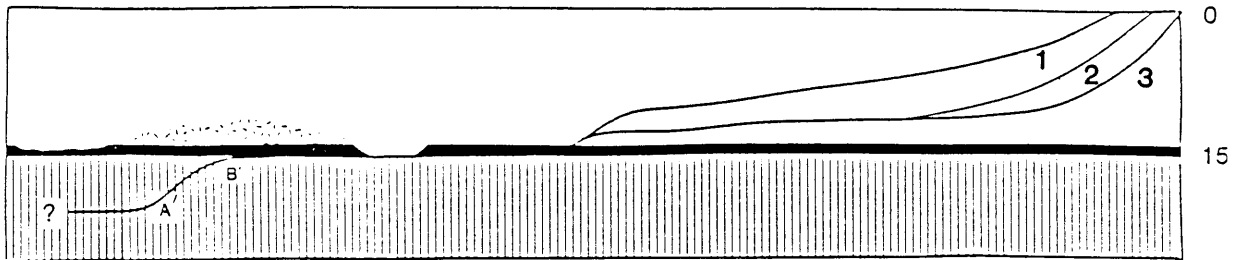
Seismic

MODEL-3



RESTORATION-3

Shortening 85 km



LEGEND

- |                         |   |             |     |
|-------------------------|---|-------------|-----|
| High Grade Gneisses     | — | Anorthosite | ⋯⋯⋯ |
| Mid-Lower Crustal Rocks |   | Fault       | —   |

Figure 7.4: Model 3: Faults 1 and 3 each with significant displacement totaling in 85 km of shortening.

## Summary of Chapter 7

Using geometric constraints from the seismic data, the surface geology, and the available geobarometry on the vertical uplift of the high grade gneisses, three restorations of the southern cross section have been proposed. Depending on which of the faults is the principal detachment and where potential ramps are placed, estimates of the minimum amount southeast directed shortening associated with the formation of the KSZ range between 55-85 km.

On a regional scale the crustal geometry of the Chapleau block is generally well constrained; however without additional seismic data, the northwest continuation of the ILFZ surface is undetermined and therefore the exact mechanism of crustal deformation that caused the KSZ can not be fully understood. For example, in order to accommodate this magnitude of overthrusting within the upper and middle crust, the lower crust and upper mantle must have also been shortened. Such deeper level shortening could be accommodated by either extending the detachment(s) to an ancient plate boundary possibly located somewhere in the northwestern Superior province (Geis et al, 1989), or by ductile flow and crustal thickening in the lower crust beneath the KSZ (Percival et al, 1989). In either case,

however, a substantial amount of contraction took place; thus, regardless of the mechanism of deformation it is clear that a large portion of the Superior province has been detached during the formation of the KSZ.

## CHAPTER-8: CONCLUSIONS

Regional and high resolution seismic reflection profiles have imaged the faults responsible for the emplacement of the granulite and amphibolite grade rocks of the Kapuskasing structure zone in Ontario. Along an east-west profile at least three low angle reflective zones are interpreted as southeast verging thrust faults that appear to merge into a horizontal detachment at about 3.0-3.5 s (9-12 km) that may ramp deeper into the crust. This a significant discovery because previous interpretations have suggested that the middle to lower crustal rocks have been uplifted along a high angle thrust fault that extends to depths in excess of 30 km.

Regional profiles that cross the Chapleau block in several different orientations reveal that the isochron contours of the thrust surface parallel the surface expression of the fault, the Ivanhoe Lake fault zone, and show that the thrusting was southeast-directed. If the faults continue to the northwest, this would imply that much of the upper-middle crust of the Superior province was detached from the lower crust during the formation of the KSZ. The seismic reflection geometry is similar to that seen in Phanerozoic sedimentary fold and thrust belts, such as the Rocky Mountains, with ramps, flats and imbricate

thrusts. However, the deformation of the KSZ took place in Archean amphibolite and granulite facies rocks, suggesting that deformation of such rocks occurs in a similar fashion to those in higher crustal level lower grade layered rocks.

Using the seismic geometry and the surface geology as constraints, three conceptual models have been proposed to explain the geometry. The first two models interpret the uppermost fault, fault 1, as the principal detachment, involving uplift along a staircase trajectory with at least two ramps. The third model has significant displacement along both fault 1 and fault 3, the deepest level fault. To account for the 15-17 km of vertical uplift of the Kapuskasing granulites, values of estimated horizontal shortening range between 55-85 km in the NW-SE direction. The estimates of shortening depend on where ramps are placed.

Large structures are imaged in the adjacent Abitibi belt. On a regional scale these features roughly parallel the surface expression of the Ivanhoe Lake fault zone, suggesting that either they had some influence on the location of the KSZ, or that they are possible deeper level detachments that were formed at the same time as the Kapuskasing uplift and that project south and east into the Abitibi belt.

Reprocessing of regional line 2 revealed that a prestack summation of adjacent shot gathers has little affect on the

stack section and cannot account for the apparently inferior image of the original regional section as compared to the high resolution section. Conventional reprocessing of the regional data with only the near offsets (less than 2.5 km) and a correlation statics window that encompasses early times produces a section that is structurally comparable to the high resolution profile. Pre-stack spectral balancing provides additional improvement in the regional data.

### **Recommendations for Future Work**

The analysis of the seismic data so far has provided a wealth of new information on the subsurface geometry of the KSZ; however, it has also presented some new questions concerning the structure, seismic character and evolution of this rare geologic feature. Thus, there are many exciting opportunities for future geophysical and geological research in the KSZ and adjacent regions. As a result of this work, several recommendations can be made for additional analysis of the existing seismic data; some of these are mentioned here.

The results from the reprocessing of regional line 2, suggest that the images from the other regional profiles can be substantially improved by similar careful reprocessing.

This will likely improve the correlation of the faults with the surface features on lines 1, 5 and 6 and allow for more accurate mapping of the 3-D structure of the Chapleau thrust block. Further processing should also be done on the high resolution data. An attempt should be made to extract more shallow information to improve the ties with the surface geology. Also, the processing of the data recorded with inline horizontal geophones should be done. Although preliminary analysis of shot gathers shows very little reflected energy, future filtering may extract converted shearwaves, which will likely provide useful rock property information. If a follow-up seismic program is done, some additional lines should be acquired across the ILFZ to further constrain the position of the faults in the subsurface. Other possibilities for future lines would include extending the survey further to the northwest in attempt to determine what happens to the detachments in the deeper crust. Further investigation of the structures imaged within the Abitibi belt should be done by making an attempt to tie them to surface features. More detailed surface mapping may provide some insight here. Other geologically related studies should include more detailed geobarometry to provide better constraints on the vertical uplift between the KSZ and surrounding areas.



**REFERENCES**

Bally, A.W., Gordy, P.L. and Stewart, G.A., 1966, Structure, seismic data, and orogenic evolution of the southern Canadian Rockies: Bull. Can. Petr. Geol., 14, p. 389-411.

Barazangi, M. and Brown, L. (editors), 1986a, Reflection Seismology: A Global Perspective: Am. Geophys. Un. Geodyn. Ser., 13: 311 p.

Barazangi, M. and Brown, L. (editors), 1986b, Reflection Seismology: The Continental Crust: Am. Geophys. Un. Geodyn. Ser., 14: 339 p.

Boland, A.V. and Ellis, R.M., 1989, Velocity structure of the Kapuskasing Uplift, Northern Ontario, from seismic refraction studies: J. Geophys. Res., p.7189-7204.

Boyer, S.E., and Elliott, D., 1982, Thrust systems: Am. Assoc. Petr. Geo. Bull., v. 66, p. 1196-1230.

Brown, G.C., and Mussett, A.E., 1984, The Inaccessible Earth: George Allen and Unwin Pub., London.

Burnsall, J.T., 1989, Structural sequence from the southeastern part of the Kapuskasing Structural Zone in the vicinity of Ivanhoe Lake, Ontario: in Current Research Part C, Geol. Surv. Can. Pap., 89-1C, p. 405-411.

Burke, K. and Dewey, J.F., 1973, Plume-generated triple junctions: Key indicators in applying plate tectonics to old rocks; J. Geol., 81, pp. 406-433.

Christensen, N.I. and Szymanski, D., 1988, The origin of reflections from the Brevard Fault Zone; J. Geophys. Res., 93, p. 1087-1102.

Cook, F.A., 1985, Geometry of the Kapuskasing structure from a Lithoprobe pilot reflection survey: Geology, v. 13, p. 368-371.

Coward, M.P. and Fairhead, J.D., 1980, Gravity and structural evidence for deep of the Limpopo belt, Southern Africa: *Tectonophysics*, 68, p. 31-43.

Dahlstrom, C.D.A., 1969, Balanced cross sections: *Can. J. of Earth Sci.*, 6, p. 743-757.

Dahlstrom, C.D., 1970, Structural geology in the eastern margin of the Canadian Rocky Mountains: *Bull. Can. Petr. Geol.*, v. 18, p. 332-406.

Fountain, D.M., Hurich, C.A. and Smithson, S.B., 1984, Seismic reflectivity of mylonite zones in the crust: *Geology*, 12, p. 195-198.

Fountain, D.M., and Salisbury, 1981, Exposed cross sections through the continental crust: implications for crustal structure, petrology and evolution: *Earth Planet. Sci. Lett.*, 56, p. 263-277.

Garland, G.D., 1950, Interpretation of gravimetric and magnetic anomalies on traverses in the Canadian Shield in Northern Ontario; *Publ. Dom. Observ.*, Ottawa, Rep. Vol. 16, 1, 57 pp.

Geis, W.T., Cook, F.A., Green, A.G., 1988, Preliminary results from the high resolution seismic reflection profile: Chapleau block, Kapuskasing Structural Zone: Expanded Abstract, Project Lithoprobe Kapuskasing Structural Zone Transect Workshop I, Univ. of Toronto, Feb., 1988.

Geis, W.T., Cook, F.A., Green, A.G., Percival, J.A., West, G.F., and Milkereit, B., 1989, Thin thrust sheet formation of the Kapuskasing structural zone revealed by Lithoprobe seismic reflection data: *Geology*, submitted.

Green, A., Milkereit, B., Percival, J., Davidson, A., Parrish, R., Cook, F., Geis, W., Cannon, W., Hutchinson, D., West, G., Clowes, R., 1989, Origin of deep crustal reflections: Results from seismic profiling across high grade metamorphic terranes in Canada: *Tectonophysics*, in press.

Innes, M., Goodacre, A., Weber J., and McConnell, R., 1967, Structural implications of the gravity field in Hudson Bay and vicinity: *Can. J. of Earth Sci.*, 4, p. 977-993.

Jones, T.D. and Nur, A., 1984, The nature of seismic reflections from deep crustal fault zones: *J. Geophys. Res.*, 89, p. 3153-3171.

Kong, S.M., Phinney, R.A., and Roy-Chowdhury, K., 1985, A nonlinear signal detector for enhancement of noisy seismic sections: *Geophysics*, 50, p. 539-550.

Kroner, A., (editor), 1981, Precambrian plate tectonics: Developments in Precambrian geology 4, Elsevier Sci. Pub. Co., New York.

Leclair, A.D. and Poirier, G.G., 1989, The Kapuskasing uplift in the Kapuskasing area, Ontario: in Current Research, Part C, *Geo. Surv. Can. Pap.* 89-C, p. 225-234.

McGlynn, J. C., 1970, The Superior Province, In R.J.W. Douglas (Ed.) *Geology and Economic Minerals of Canada*, edited by R.J.W. Douglas, *GSC Econ. Geo. Rep.*, 1 pp. 59-71.

Milkereit, B., and Spencer, C., 1988, Noise suppression and coherency enhancement of seismic data: Presented at the Colloquium on "Statistical Applications in the Earth Sciences", Ottawa, 14-18 November, 1988.

Moser, D., 1989, Mid-crustal structures of the Wawa gneiss terrane near Chapleau, Ontario: in Current Research, Part C, *Geol. Surv. Can. Pap.*, 89-1C, p. 215-224.

Neidell, N.S. and Taner, M.T., 1971, Semblance and other coherency measures on multichannel data: *Geophysics*, 36, 482-487.

Nisbet, E.G., 1987, *The Young Earth: An Introduction to Archaean Geology*: Allen and Unwin, Pub.

Percival, J.A., 1983, High grade metamorphism in the Chapleau-Foleyet area, Ontario: *Amer. Min.*, 68, p. 667-686.

Percival, J.A. and Card, K.D., 1983, Archean crust as revealed in the Kapuskasing uplift, Superior Province, Canada: *Geology*, v. 11, p. 323-326.

Percival, J.A. and Card, K.D., 1985, Structure and evolution of Archean crust in central Superior Province, Canada: in: Ayres, L., Thurston, P.C., Card, K.D. and Weber, W., eds. *Evolution of Archean Supracrustal Sequences*, Geol. Ass. Can., Spec. Pap., 28, p. 179-192.

Percival, J.A. and Fountain, D.M., 1989, Metamorphism and melting at an exposed example of the Conrad discontinuity, Kapuskasing uplift, Canada: in Bridgewater, D. ed. *Fluid Movements, Element Transport and the Chemical Composition of the Crust*. NATO Advanced Studies Institute. Kluwer Academic Publishers, Dordrecht, in press.

Percival, J.A. and Green, A.G., 1989, Towards a balanced crustal scale cross section of the Kapuskasing uplift, Expanded Abstract, Project Lithoprobe Kapuskasing Structural Zone Transect Workshop II, Univ. of Toronto, Nov., 1989.

Percival, J.A., Green, A.G., Milkereit, B., Cook, F.A., Geis, W.T., West, G.F., 1989, Lithoprobe Reflection Profiles Cross exposed Deep Crust: Kapuskasing Uplift: Nature, submitted.

Percival, J.A. and McGrath, P.H., 1986, Deep crustal structure and tectonic history of the northern Kapuskasing uplift of Ontario: An integrated petrological-geophysical study: *Tectonics*, v. 5, p. 553-572.

Percival, J.A., Parrish, R. Krogh, T. and Peterman, Z., 1988, When did the KSZ come up?, Expanded Abstract, Project Lithoprobe Kapuskasing Structural Zone Transect Workshop I, Univ. of Toronto, Feb., 1988.

Raase, P., Raith, D., Ackermann, D., Lal, R.K., 1986, Progressive metamorphism of mafic rocks from greenschist to granulite facies in the Dharwar craton of south India: *J. Geol.*, 94, p. 261-282.

Riccio, L., 1981, Geology of the northeastern portion of the Shawmere anorthosite complex, District of Sudbury: Ontario Geological Survey Open File Report 5338, 113p.

Simmons, E.C., Hanson, G.N. and Lumbers, S.B., 1980, Geochemistry of the Shawmere anorthosite complex, Kapuskasing structural zone, Ontario: Precambrian Research, 11, 43-71.

Taner, M.T., Koehler, F., and Alhilali, K.A., 1974, Estimation and correction of near surface time anomalies: Geophysics, 39, p. 441-463.

Watson, J., 1980, the origin and history of the Kapuskasing structural zone, Ontario, Canada; Can. J. of Earth Sci., V. 17, pp 866-875.

Wilson, J.T., 1968, Comparison of the Hudson Bay Arc with some other features; in Science, History and Hudson Bay edited by C.S Beals, Dept. of Energy Mines and Resources, Ottawa, pp. 1015-1033.

Yilmaz, O., 1987, Seismic Data Processing: Investigations in Geophysics No. 2: Society of Exploration Geophysicists, Tulsa.